University of New Mexico
UNM Digital Repository

Civil Engineering ETDs | Engineering ETDs

8-27-2012

Quantifying the contribution of bank storage due to an alteration in stream stage

Jeffrey Samson

Follow this and additional works at: https://digitalrepository.unm.edu/ce_etds

Recommended Citation
Samson, Jeffrey. "Quantifying the contribution of bank storage due to an alteration in stream stage." (2012).
https://digitalrepository.unm.edu/ce_etds/71

This Thesis is brought to you for free and open access by the Engineering ETDs at UNM Digital Repository. It has been accepted for inclusion in Civil Engineering ETDs by an authorized administrator of UNM Digital Repository. For more information, please contact disc@unm.edu.

www.manaraa.com

Jeffrey Eric Samson
Candidate

Civil Engineering
Department

This thesis is approved, and it is acceptable in quality and form for publication.

Approved by the Thesis Committee:

Dr. Mark Stone, Chairperson

Dr. John Stormont

Dr. Gary Weissmann

www.manaraa.com

QUANTIFYING THE CONTRIBUTION OF BANK STORAGE DUE TO AN ALTERATION IN STREAM STAGE

BY

JEFFREY ERIC SAMSON

Bachelor of Science
College of Education
New Mexico State University, 2003

Master of Arts
College of Education
Arizona State University, 2005

Submitted in Partial Fulfillment of the
Requirements for the Degree of

Master of Science
Civil Engineering

The University of New Mexico
Albuquerque, New Mexico

July, 2012

www.manaraa.com

ACKNOWLEDGEMENTS

First and foremost I'd like to thank my family for their love and support throughout this process. A change of careers is not always as easy as I have experienced, and that is due to my wife and son.

I'd also like to acknowledge the support and guidance I have received from everyone at UNM. This includes my advisor, Dr. Mark Stone, and committee members Drs. John Stormont and Gary Weissmann. This also includes Dr. Laura Crossey, the PI for the NSF LSAMP fellowship, which funded my degree.

Finally, I could not have completed this work without the help of my good friends, Robert Trujillo, Abdou Harissou Ouro Bang'na Nassam, and Stephen Brown. Through our conversations, interactions, and time in the field, I have gained much knowledge, many laughs and good memories.

I have truly enjoyed every step of this experience. I have met some amazing people, made some great friends, and learned more than I ever imagined I would when I first stepped on this path. I am humbled by the many great minds around me, and I look forward to focusing my expertise toward the important environmental issues of our day.

* * * * * * * * * * * *

In the end
we will conserve only what we love,
we will love only what we understand,
we will understand only what
we are taught.

-Baba Dioum

www.manaraa.com

QUANTIFYING THE CONTRIBUTION OF BANK STORAGE DUE TO AN ALTERATION IN STREAM STAGE

BY

JEFFREY ERIC SAMSON

B.S. EDUCATION, NEW MEXICO STATE UNIVERSITY, 2003

M.A. MATHEMATICS EDUCATION, ARIZONA STATE UNIVERSITY, 2005

M.S. CIVIL ENGINEERING, UNIVERSITY OF NEW MEXICO, 2012

ABSTRACT

The desire to control rivers to reduce risks of flooding while providing water storage for municiplan and agricultural uses has resulted in the disconnection of rivers from their floodplains. An important and often neglected outcome of this detachment is the loss of a plethora of important ecosystem services. This research was focused on answering the following questions related to riparian groundwater storage (bank storage): 1) What is the time to saturation (maximum storage) and time to release of bank storage water as the result of a flood pulse that overbanks a portion of the floodplain?; 2) How does soil stratigraphy impact the movement of water within the floodplain?; and 3) How has historical river engineering and management influenced these processes?. The study was conducted on a site in the Rio Grande floodplain in Albuquerque, New Mexico. This site has been the focus of two recent studies which aided in the understanding of the system, and they have both yielded data that was utilized in the model development and calibration of this study. The research questions were answered through a combination of field observations and numerical modeling exercises. The field analysis focused on determining the necessary hydraulic properties that govern water movement through soil.

www.manaraa.com

The evaluated properties included saturated hydraulic conductivity, particle size distribution, as well as the development of water retention curves. The results of this laboratory work were used as inputs for a two-dimensonal grounwater model (HYDRUS-2D), which was used to quantify bank storage under a variety of scenarios. Multiple scenarios were studied to answer the research questions; these included variations in the flood stage, flood duration, and variations to the alluvial architecture. Results show bank storage is dominated by horizontal flow through the alluvial aquifer and thus water movement is highly sensitive to floodplain stratigraphy. Also, the highly engineered river system of the middle Rio Grande valley has resulted in the diminished capacity of the floodplain to store water for a prolonged period of time.

www.manaraa.com

Table of Contents

www.manaraa.com

List of Figures

www.manaraa.com

www.manaraa.com

List of Tables

www.manaraa.com

Introduction

"Rivers throughout the world have suffered a long history of degradation through direct and indirect human influence" (Maddock, 1999). The desire to control rivers to reduce risks of flooding while providing storage for urban and agricultural use has resulted in the disconnection of rivers from their floodplains. In many river systems throughout the world, and in particular in the southwestern United States, river management strategies have focused on confining the waterway to a predefined size and capacity to allow for the maximum amount of developable or agricultural land (ASFM, 2008). It is also known that "the structure, function, and composition of riparian ecosystems are dependent upon episodic disturbances such as those caused by infrequent high flows" (Tetra Tech Inc., 2004). An important and often neglected outcome of this detachment is the loss of a plethora of important ecosystem services that include: (1) the improvement of water quality (Wilson and Carpenter, 1999; de Groot et al., 2002); (2) the decreased potential for devastating fires through the mobilization of stagnant organic matter while also supporting the base of the food web through the mobilization of substantial quantities of plant nutrients into the stream (Molles et al., 1998); and (3) most importantly for the purpose of this paper, an increase in the quantity of bank storage water helps to attenuate flood events (Sophocleuos, 2002; Whiting and Pomeranets,1997), while also supporting base flows as the hydraulic gradient is reversed due to the stream stage recession (Bates et al., 2000; Squillace, 1996).

The objective of this study was to improve understanding of the physical process of bank storage in an alluvial floodplain system. Specifically, the processes of water movement and storage were investigated at a study site in the Rio Grande Bosque in Albuquerque,

www.manaraa.com

New Mexico, USA. The research objective was met by answering the following three questions: 1) what is the time to saturation (maximum storage) and time to release of bank storage water as the result of a flood pulse that overbanked a portion of the floodplain?; 2) how does soil stratigraphy impact the movement of water in the floodplain?; and 3) how has historical river engineering and management influenced these processes? These questions were addressed using a combination of field measurements and a numerical model to quantify the movement of water, and subsequent storage, under a range of streamflow and stratigraphic conditions.

Previous Research

The process of bank storage water entering and then leaving a floodplain has been studied by many researchers in the laboratory setting (Todd, 1955), analytically (Rorabaugh, 1963; Cooper and Rorabaugh, 1963; Moench et al., 1974; Morel-Seytoux, 1975; Hunt, 1990; Barlow et al., 2000; Hantush et al., 2002; Hunt, 2005) and through numerical modeling (Pinder and Sauer, 1971; Squillace, 1996; Whiting and Pomeranets, 1997; Bates et al., 2000; Chen et al., 2006; Li et al., 2008). Todd (1955) was one of the first researchers to study the effects of bank storage due to an increased stream stage. He used a Hele-Shaw viscous fluid model to quantify bank storage for what he recognized as a simplified and idealized system. Through his research, Todd concluded that the volume of ground water recharge is directly proportional to the amplitude and duration of the event. He also concluded that the majority of bank storage occurs within a close proximity to the bank (75% within 120 m), and that measurable return flow persisted for weeks after the stream stage had receded.

www.manaraa.com

Rorabaugh (1963) analytically studied bank storage effects relative to a fluctuating river and used his results to provide a basis for forecasting the ground water contribution to streamflow during low-flow periods. Cooper and Rorabaugh (1963) presented an analytical solution to bank storage in response to stream stages that followed a family of sinusoidal patterns. They concluded that the release of bank storage water can take considerable time with a significant amount of water remaining stored in the banks at ten flood periods after the flood recession. Moench et al (1974) utilized the convolution approach to analytically study stream-aquifer interactions. First the open channel problem was solved using the unit response method, and then these results were modified for ground water interaction based upon the linear diffusive flow equation developed by Cooper and Rorabaugh (1963). Morel-Seytoux (1975) derived the equations to numerically predict the 2D evolution of an aquifer, the wave propagation in a channel, and the interaction between both.

More recently, Hunt (1990) developed an analytical approximation for the bank storage effect in flood waves through the use of a perturbation approach that combined the St. Venant equations for open channel flow with the Dupuit approximation for aquifer flow. His results reinforced the findings of previous researchers that bank storage delays the arrival of the flood wave, depresses the peak, and adds to the tail of the flood hydrograph as the flood recedes. Later, Hunt (2005) analytically compared 2D solutions to groundwater storage to 1D Dupuit solutions for an unconfined aquifer adjacent to a stream. The 2D solution is more robust in that it includes vertical velocity components and aquifer elasticity, but the results show the simpler Dupuit solutions give reasonable approximations for storage under most conditions. The simplified Dupuit assumptions

www.manaraa.com

did not provide accurate results for scenarios with large aquifer depth to width ratios as well as large anisotropy ratios.

Barlow and Moench (2000) developed analytical step response functions to calculate bank storage, as well as aquifer heads and seepage rates that occur in response to stream-stage fluctuations. They developed two computer models based on the step response function and convolution integrals to study surface and ground water interactions. When compared to actual field data, their results matched up very well with results generated by a more complex numerical model. Hantush (2002) developed analytical solutions that utilized impulse response functions to relate stream outflow, stream-aquifer flow, bank storage, and cumulative reach discharge volume to inflow hydrographs using convolution integrals. These studies have provided insight into the process of bank storage but the applicability of these results is reliant on a solid understanding of the necessary parameters. However the assumptions of aquifer homogeneity or fully penetrating streams, which allow for many of the solutions to be derived, can decrease the accuracy of the estimated bank storage (Sharp Jr., 1977). Also, the Dupuit-Forchheimer conditions that are present in nearly all analytical bank storage models is a main source of error because ground water flow is not essentially horizontal; especially in the vicinity of the stream where flow is dominated by vertical flow components (Sharp Jr., 1977).

On the numerical side of bank storage analysis, Pinder and Sauer (1971) studied the effects of bank storage due to a flood wave through the development of a model that simultaneously solved the equation for one-dimensional open channel flow with the two-dimensional transient ground water flow, while also incorporating an expression for flow through the wetted perimeter. They concluded, similarly to Todd (1955) and Hunt (1990),

www.manaraa.com

that bank storage can have significant impacts on flood attenuation by 1) delaying the arrival time of the flood, 2) by dampening the peak flow, and 3) by extending the flood hydrograph through delayed return flows. They also found that the length of the channel as well as the degree of connectivity between the stream and floodplain aquifer can have a considerable impact on bank storage. Along with Todd (1955) and Zitta and Wiggert (1971), Pinder and Sauer were able to determine that the majority of bank storage occurs within a close proximity to the stream because the flood wave which propagates through the system decreases rapidly as the distance from the stream increases.

Squillace (1996) was one of the first to combine field monitoring with the construction of a two-dimensional groundwater flow model that accurately simulated the observed environment to quantify the movement of the bank storage water at the Palisades adjacent to the Cedar River, Iowa. The numerical modeling results of Squillace (1996) showed that bank storage caused the groundwater flux to the river to increase by a factor of five during the first three weeks of baseflow after runoff and that it required about five weeks of baseflow for bank storage water to discharge from the alluvial aquifer after the peak river stage. He found that a 2-meter rise in stream stage resulted in at least a 30-meter pulse into the banks. Whiting and Pomeranets (1997) constructed a numerical model based upon the work of Neuman and Witherspoon (1970) to quantify bank storage. They found that the total volume of water that can be stored during events with increased stream stage is proportional to the width of the aquifer, the height of the bank, and the specific yield of the sediments; while the temporal component of the desaturating pores depends on the floodplains width and the hydraulic conductivity of the sediments (Whiting and Pomeranets, 1997). Chen et al. (2006) developed a 3-dimensional transient

www.manaraa.com

ground water model to study the characteristics of baseflow and baseflow separation due to fluctuations in stream stage under an array of flooding conditions. Their model incorporated a range of scenarios that analyzed baseflow in heterogeneous and anisotropic aquifers, along with variations to streambed hydraulic properties and hydraulic gradients. They determined that bank storage is sensitive to both the rate the flood pulse raises and aquifer/streambed conductivity. Aquifers with lower conductivities (5m/d) stored 24% of an aquifer with higher conductivities (100m/d), and aquifers with large anisotropy ratios stored less water as well and released the water over a longer period of time.

Li et al. (2008) used numerical simulations to quantify bank storage of a variably saturated, homogeneous, anisotropic, unconfined aquifer abutting a stream during a flood period. The stream was assumed to be fully penetrating with perfect hydraulic connection at the banks, and the stream bed was also assumed to be impermeable. Li et al. (2008) improved on previous work by simultaneously incorporating the nonlinear effects of a variable seepage face along with the gradually varying water saturation in the unsaturated zone. Through their efforts they found that bank storage is sensitive to both the aspect ratio and the anisotropy ratio of the aquifer. If the product of these two parameters was greater than 10, than bank storage was small because the pore space was already saturated due to the significant seepage face. However, if the product was small then the capillary fringe plays an important role in bank storage. For soils with strong capillary forces the normalized bank storage was negligible, whereas storage for soils with mild or weak capillary effects reached approximately 25% to 55.4% respectively.

www.manaraa.com

Researchers have primarily focused on bank storage as the result of an increase in stream stage which stayed within the confines of the stream banks. These studies did not address the more complex influence of hill slope or inundated floodplain dynamics (Bates et al., 2000). Bates et al. (2000) combined field monitoring with numerical modeling to study the floodplain and channel interactions for a lowland river. Their objective was to determine the contribution of bank storage to river flows over several months following an instantaneous drop in water level. In the process they developed ESTEL, a 2-D finite element model of saturated-unsaturated flow, which simulated the field monitored environment reasonably well. They concluded that floodplain hydrology is predominantly a two-dimension (lateral) process, and that three-dimensional effects become more significant at the beginning and end of each event (Bates et al., 2000). Despite the limitations of their study, the combination of field work and modeling proved to be a powerful tool with which to undertake process investigations in floodplain environments (Bates et al., 2000).

Numerical methods, by necessity, have their own shortcomings; these being primarily focused around the amount of aquifer data necessary to develop an accurate and calibrated model. Therefore, a numerical model studying bank storage requires a large data set that defines the hydraulic parameters of the system. From this brief review of previous work it can be seen that much effort has been put towards understanding bank storage due to an in-stream flood event. The majority of these researchers approached the problem with the goal of hydrograph separation to aid in the understanding of floodwave modification. This differs from the approach of this study that quantified bank storage to highlight an important ecosystem process (overbank flooding) that represents the

www.manaraa.com

lifeblood of (southwestern) riparian corridors; which also provide the highest concentrations of plant an animal communities thus maintaining a stable source of biodiversity (ASFM, 2008).

Methods

Site description

This research took place in a section of the Middle Rio Grande, located just north of Rio Bravo Boulevard in Albuquerque, New Mexico (Figure 1). In the Albuquerque area, the sedimentary deposits form an extensive shallow aquifer which represents the last cut and fill cycle of the Rio Grande fluvial system (Rankin et al., 2011), and are composed of "unconsolidated to poorly consolidated, pale brown, fine to coarse grain sand and rounded gravel with subordinate, discontinuous lenoidal interbeds of fine grained sand, silt and clay" (Connell et al., 2007). This description characterizes an extremely heterogeneous alluvial aquifer which is the product of thousands of years of major flood events and soils deposition. The location of this study was chosen because of its proximity to two recent studies that yielded data which aided in the understanding of the site. Engdahl et al. (2010a, 2010b) studied the impact of lithologic heterogeneity on transport rates and river flow loss, and the USGS has been investigating the surface water/ground water

Figure 1. Rio Bravo site location with wells (open circles) and surface water gauges (cricles with black cneters).

www.manaraa.com

interactions through the installation of a series of nested piezometers and stream gauges at this location since 2003 (http://nm.water.usgs.gov/projects/riograndesections). At this reach the river is paralleled by levees and drains on either side. The purpose of these riverside drains is to intercept lateral ground water flow from the river while also preventing waterlogged soil conditions in the valley (Rankin et al., 2011).

The drains were constructed by the Middle Rio Grande Conservancy District (MRGCD) during the 1920s and 1930s as a result of increased sedimentation (primarily silt) due to development and deforestation upstream in the watershed dating back to the 1880s (MRGCD website). The high water table, which was produced due to sedimentation, led to saline soils and the conversion of 24,300 hectares of farmland into wetlands and salt grass fields (MRGDC website). Due to these conditions, by 1935 the MRGCD built a total of 1315 kilometers of new drains along with levees and a system of jetties that helped to lower the water table while converting the river into a channel and a perennial losing stream in the Albuquerque reach. However, these efforts were not enough to control the river during major floods in 1941 and 1942. This led the MRGCD to enlist help from the federal government, and out of the flood control acts of 1948 and 1949, millions of dollars were spent on the construction of dams upstream along with increased channelization efforts. The end result is a Rio Grande and its riverside drains which are so intimately related that they function as a single system (Bartolino and Cole, 2002).

Figure 2 shows a profile view of the Rio Bravo cross-section, which is the focus of this study. The floodplain on the east side of the river was chosen for this work because of its size, ease of access, and availability of data. An interesting feature at this location is the presence of a two-tier floodplain. Initially, the lower level was thought to be the natural

www.manaraa.com

remnants of an old streambed with the upper level representing a terrace of which the river no longer floods. However, upon further research it was found that the lower level is the result of an anthropogenic channel cut through the area prior to 1935 (see appendix A for a description of the river's evolution at this site). The river is now incised due to the efforts detailed above and the lower floodplain surface now serves as the primary floodplain where overbank flooding occurs only during periods of substantial flows. This flooding has resulted in a thick flora consisting of willow, salt cedar, Russian olive and a few cottonwoods which cover the majority of the lower level at this site. It is believed that the upper surface has not been inundated since the 1941 and 1942 floods.

Cores retrieved by the USGS during the installation of wells at this location detail a lithology composed of a series of layers. The surface was characterized as a muddy layer to a depth of 1.5m, which was underlain by a series of layers composed of sands, pebbles, and gravels to a depth of 15.2 m (Engdahl et al., 2010b). An analysis of the cores for the wells included in this study is included in Appendix E.

Field Study

Field investigations were undertaken to quantify the hydraulic properties of the near-surface soils. At sites 1-4, shown in Figure 2, a pit was excavated down to the water table so that samples could be gathered for laboratory analyses. Pictures of the field work and the findings can be found in Appendix B. Sites one and two, located 50 meters apart on the lower floodplain, were composed of 4 alternating soil layers above the water table to a depth of 0.4 m and 0.73 m respectively. Sites three and four, located 47 m apart on the upper floodplain, were composed of six alternating soil layers above the water table to a depth of 1.83 m and 1.91 m respectively. At all four sites the alternating layers displayed

www.manaraa.com

the same pattern of a surface layer composed of fines, underlain by a coarse layer dominated by sands. This fine to coarse pattern continued down to the water table where a sandy layer was present. Figure 3 details the observed layers used in the model.

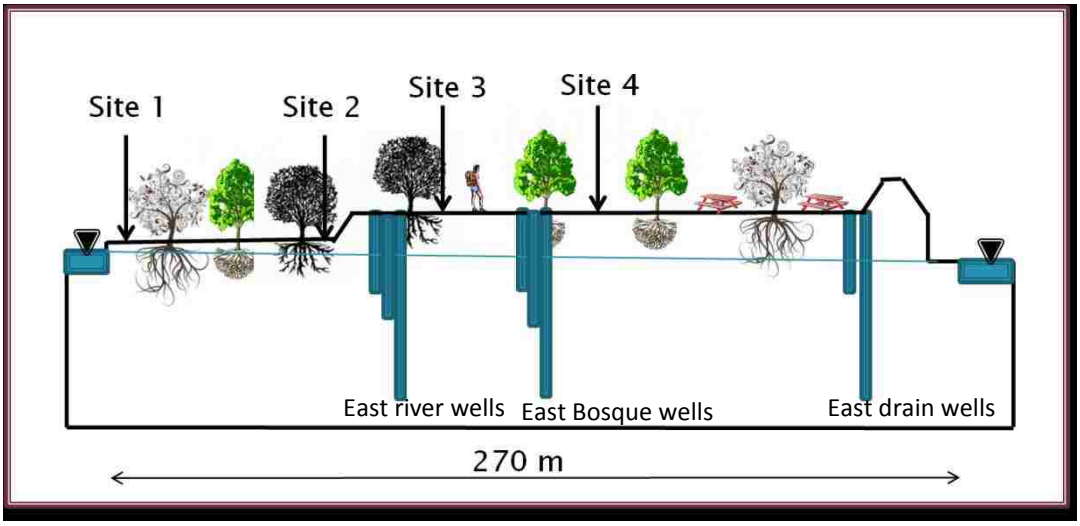

Figure 2. Profile schematic of Rio Bravo cross-section along with the relative locations of the four locations where field work took place and the location of the nested wells

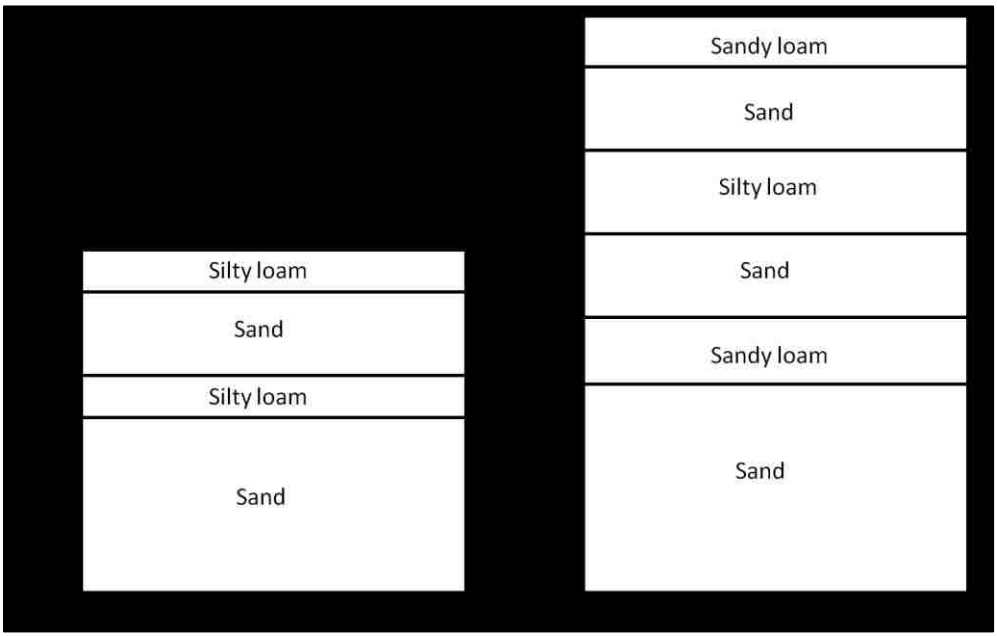

Figure 3: Layering used in model for lower and upper floodplains, including the soil type based upon the NRCS soil classification system

www.manaraa.com

Sediment samples were taken from each layer to determine their particle size distribution, in situ volumetric water content, and specific gravity. Horizontal core samples were taken from each layer that was thicker than 7 cm to determine the saturated hydraulic conductivity and the dry density. Also, samples were taken from layers that had enough moisture to maintain the soil stability to create a water retention curve. Pictures of the laboratory work can be found in Appendix C. A detailed description of the results of these laboratory analyses is included in Appendix E. Table 1 summarizes the key results for characterizing the soils. The majority of these properties align well with those detailed on the NRCS website (http://www.mo10.nrcs.usda.gov/references/guides/). The dry densities of layers two and four for site two and layer five of site four show are lower than the range, but this could very well be attributed to a miscalculation of the total volume.

Table 1. Summary of field data and laboratory results and the model K_{sat}

Site	Layer	Thickness (cm)	Percent fines (0.75mm>)	Dry Density (g/cm^3)	Volumetric water content (cm^3/cm^3)	Lab K_{sat} (cm/s)	Model K_{sat} (cm/s)
1	1	5	36.7	1.53	0.21		0.00123
	2	7.5	2.7	1.63	0.13	0.0148	0.015
	3	5	24.2	1.45	0.20		0.0024
	4	22.5	0.2	1.58	0.41	0.023	0.018
	0	20	2.5				
2	1	8.9	33.9	1.09	0.41	0.00014	0.00123
	2	30.5	0.5	1.45	0.30	0.015	0.015
	3	8.9	34.8	1.21	0.38	0.0024	0.0024
	4	2.5	0.6	1.31	0.40	0.018	0.018
3	1	14.25	20.6	1.56	0.05	0.0003	0.0013
	2	30.5	3.6	1.55	0.03	0.0038	0.0046
	3	14.5	28.2	1.38	0.22	0.00013	0.0013
	4	24	0.5	1.50	0.19	0.016	0.013
	5	21					0.00002
	6	78.75	0.6	1.50	0.37	0.017	0.017
4	1	22.9	19	1.53	0.17	0.00013	0.0013
	2	30.5	3.8	1.50	0.05	0.0055	0.0046

www.manaraa.com

3	21.6	35.6	1.42	0.30	0.00012	0.0013
4	15.25	6.3	1.39	0.15	0.013	0.013
5	12.7	38.3	1.27	0.32	0.0000023	0.00002
6	86.25	0.4	1.31	0.36	0.017	0.017

Model development

HYDRUS-2D, a finite element-finite difference numerical unsaturated flow model, was chosen to study the process of bank storage. The model utilizes Richard's Equation (a nonlinear partial differential equation) and allows for a heterogeneous soil structure and a range of soil hydraulic properties (Thompson, 2003). HYDRUS-2D incorporates the use of a triangular finite element mesh which allows for complex geometries to be modeled. A detailed description of the mesh and model parameters is included in Appendix D. In the development of this model a total station survey was utilized to obtain accurate topography of the surface structure. However, due to the thick flora located on the lower floodplain, limited sight distance did not permit a complete survey of the cross section.

The boundary conditions for the model are displayed below in Figure 4. The conditions for the stream and drain side of the model were time variable heads (TVH) and for the calibration scenario were obtained from hourly data collected by the USGS during a 2006 flood that passed through the site. The event took place on July 9th and was the result of a storm event that raised the river stage 2-feet in a matter of two hours. The flux through the base of the model was calculated using the nested piezometers located at the site, in tandem with hydraulic conductivities determined through slug tests at a location 50 meters upstream (Myers, 2010). The values calculated using this method were compared to a value obtained through a USGS study (Bartolino and Niswonger, 1999) that focused on the Rio Grande's vertical flux through heat tracers at this site and were found to be

www.manaraa.com

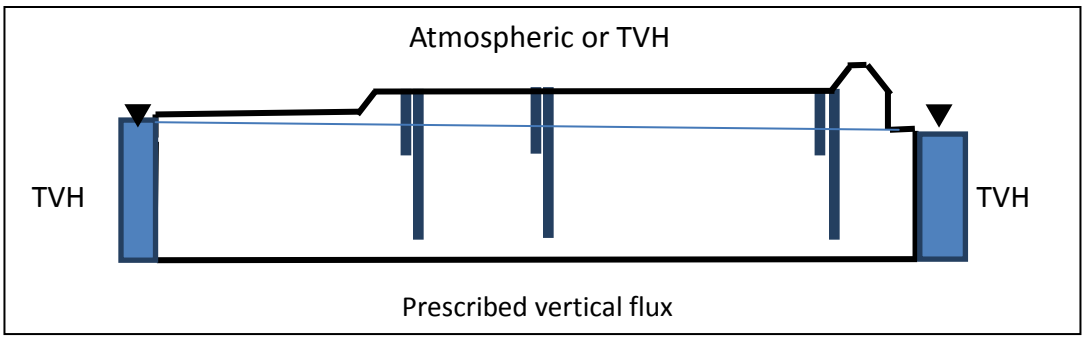

Figure 4. Conceptual model displaying the boundary conditions for the HYDRUS-2D model

within one order of magnitude of their estimates. The TVH at the surface was relative to the flood stage, and the atmospheric flux was estimated from data for the Rio Grande published by the National Riparian Service Team (Wyman, 2007). The in situ water contents shown in Table 1 were unusually low due to the absence of precipitation for a period of over 100 days prior to the excavation of the site 3 in July 2011. Site 3 was the first site to be excavated, and from the table it can be seen that the water contents in the top two layers were well below the other three sites; which is due to a rain event that shortly followed the initial field work.

The 2006 event was chosen to study bank storage since this was the only significant flood event with which there was available groundwater monitoring data. Nearly 5 cm of rain fell in the two weeks prior to the July 9th event, which would have resulted in an entirely different unsaturated near-surface soil zone. Thus, rather than using 2011 field observations of soil moisture as an initial condition, the model was run for 6 days prior to the simulated flood pulse with a gradient of water content of 0.25 to 0.43 from the surface to the water table. This period allowed the system to equilibrate to a condition that more

www.manaraa.com

closely approximated conditions in July 2006, while also reducing the impact of the initial conditions on the simulation results.

Figure 5 shows the results of the model calibration at the 50 m well. Ksat values were initially based on the laboratory experiments. This model shows a system that contains excess water when the flood began, while also storing excess water after the flood had receded. Calibration included adjustments to hydraulic conductivity and the initial conditions of the model. Originally, initial water storage was reduced by lowering the

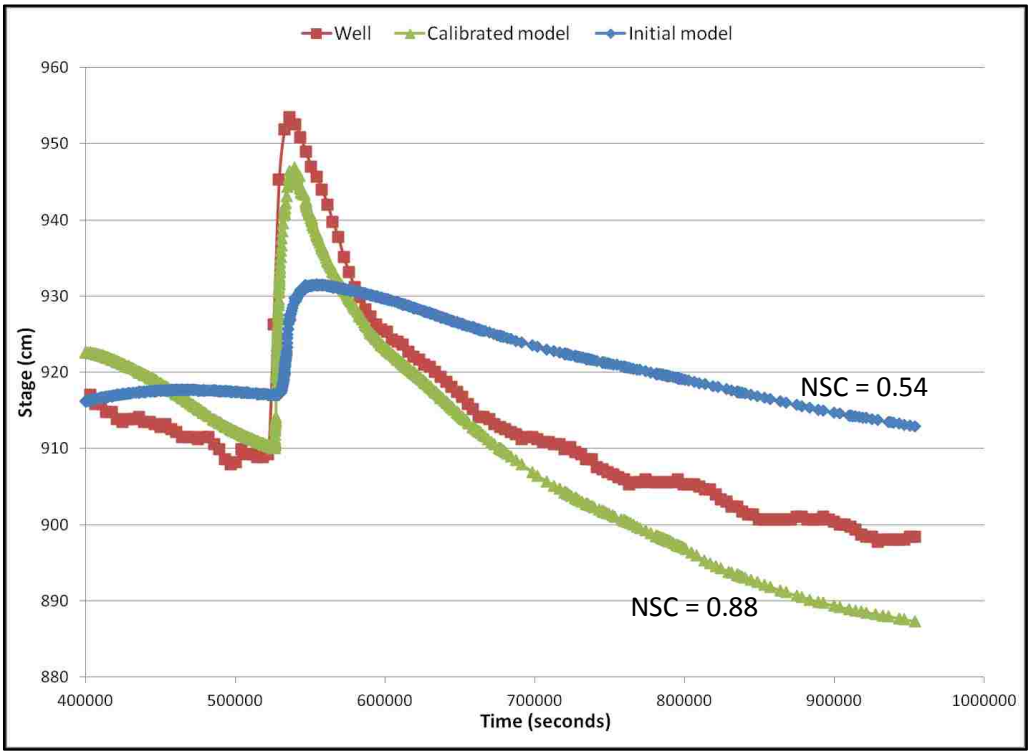

Figure 5. Model calibration results with respect to groundwater stage at the well located 50 m from the streambank, including the Nash-Sutcliffe model efficiency coefficients

water table but then the response to the flood was negligible as the water passed right through with a minimal peak. Next, the hydraulic conductivities were adjusted. These changes were made to the less permeable layers and can be seen in Table 1. These layers

www.manaraa.com

were investigated due to the uncertainty that arose due to logistic challenges in collecting field data from these locations. Given that they were clayey in nature and were dominated by fine sediments, along with roots in some cases, the sample extraction method was thought to have disrupted the samples more than the sand cores. These conductivities were changed by one order of magnitude, and the resulting curve matched up well with the observed well response to the flood. The Nash-Sutcliffe model efficiency coefficient was determined for each scenario, and the value increased from 0.54 to 0.88. This symbolizes an improved modeling of the actual conditions based up the calibration adjustments. The adjusted values were consistent with reference values for similar materials.

The model response at the 100 m well (Figure 5) did not match the observed data as satisfactory as the 50 m well. The uncalibrated model showed a minimal rise in stage. The response was increased within the calibrated model, but it still did not show a significant rise in stage. After further investigation into the well data, a similar response was observed by the East Bosque shallow well. Figure 7 shows the responses of the shallow and deep wells at each location and there is a clear anomaly that is not easily explained. Table 2 displays the calculated hydraulic gradients that existed horizontally between each site and vertically between the nested wells.

www.manaraa.com

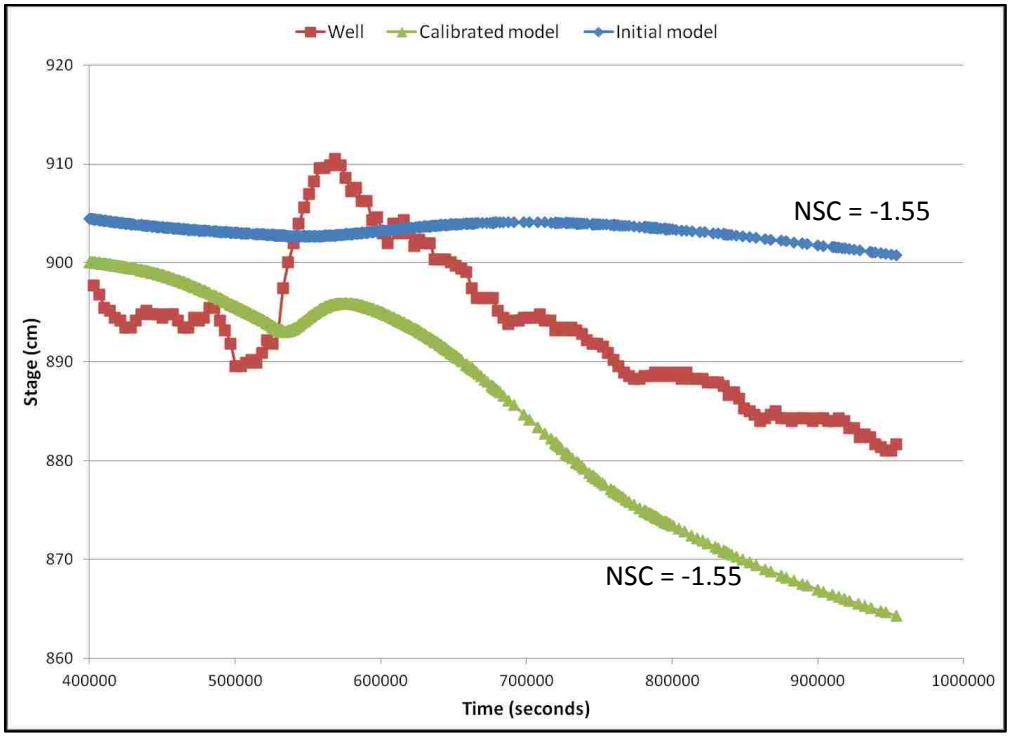

Figure 6. Model calibration results at the well located 100 m from the streambank, including the Nash-Sutcliffe model efficiency coefficients

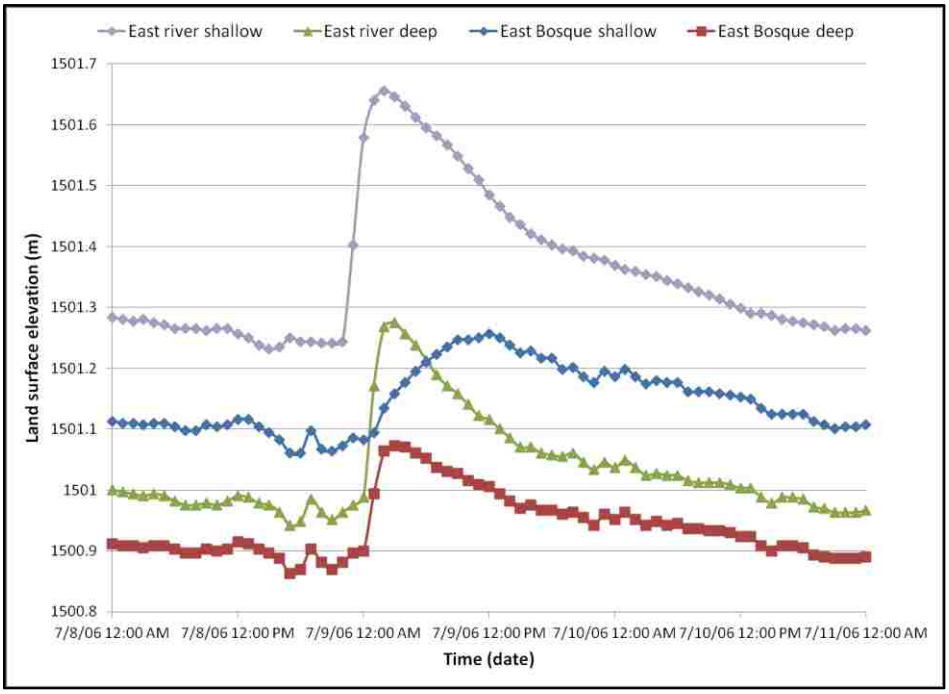

Figure 7. The observed well responses for the shallow and deep wells at the east Bosque and east river sites

www.manaraa.com

Table 2. The horizontal and vertical gradients that were present at the time of the flood

Time	Between wells			East Bosque			East river		
	Shallow gradient	Middle gradient	Deep Gradient	Shallow-middle	Shallow-deep	Middle-deep	Shallow-middle	Shallow-deep	Middle-deep
7/9/2006 1:00	0.007	0.004	0.002	0.004	0.018	0.022	0.046	0.039	0.035
7/9/2006 2:00	0.010	0.007	0.004	0.001	0.010	0.012	0.050	0.038	0.033
7/9/2006 3:00	0.011	0.009	0.004	-0.002	0.007	0.010	0.018	0.035	0.042
7/9/2006 4:00	0.011	0.010	0.004	-0.005	0.008	0.012	0.005	0.036	0.050
7/9/2006 5:00	0.010	0.010	0.004	-0.006	0.010	0.015	0.000	0.037	0.053
7/9/2006 6:00	0.009	0.009	0.004	-0.006	0.013	0.019	-0.003	0.037	0.055
7/9/2006 7:00	0.009	0.008	0.003	-0.006	0.015	0.022	-0.003	0.037	0.056

The East Bosque shallow-middle gradients are close to an order-of-magnitude less and in the opposite direction than most of the other wells. This signifies that a strong heterogeneity exists in the lithology at this location (e.g. an aquitard), which cannot be modeled accurately without further field work.

The 2006 flood pulse was used as a baseline event to understand the system's response to a flood event and bank storage at this location. Due to the brevity of the event, a decision was made to run additional hypothetical scenarios that had a larger peak stage as well as a longer flooding period once the model displayed a similar response to the known conditions. Table 3 and 4 summarize the model scenarios that were used to address the research questions.

Table 3. Six primary flooding scenarios

Event	Time to peak (hr)	Time from peak to recession (hr)	Total model run (hr)
Rio Bravo	5	26	265
Alameda	9	22	265
Rio Bravo 2-day	5	70	312
Alameda 2-day	9	66	312
Rio Bravo 10-day	5	263	505
Alameda 10-day	9	259	505

www.manaraa.com

Due to the rivers ability to naturally attenuate flood waters, the peak flowrate of the 2006 flood had decreased from 250 m^3/s (8500 cfs) at the Alameda gauge (USGS gauge 08329928) to 114.1 m^3/s (4030 cfs) at the Central gauge (USGS gauge 08330000) in a matter of 27 hours and 13.6 km (8.5 miles) of river. Two hypothetical scenarios were run to see how a larger flood might impact the Rio Bravo cross section. With this in mind, while also understanding that the upper floodplain would not be inundated, a model was run that had the flood rise and recede at the same rate with 30 cm of stage added to the

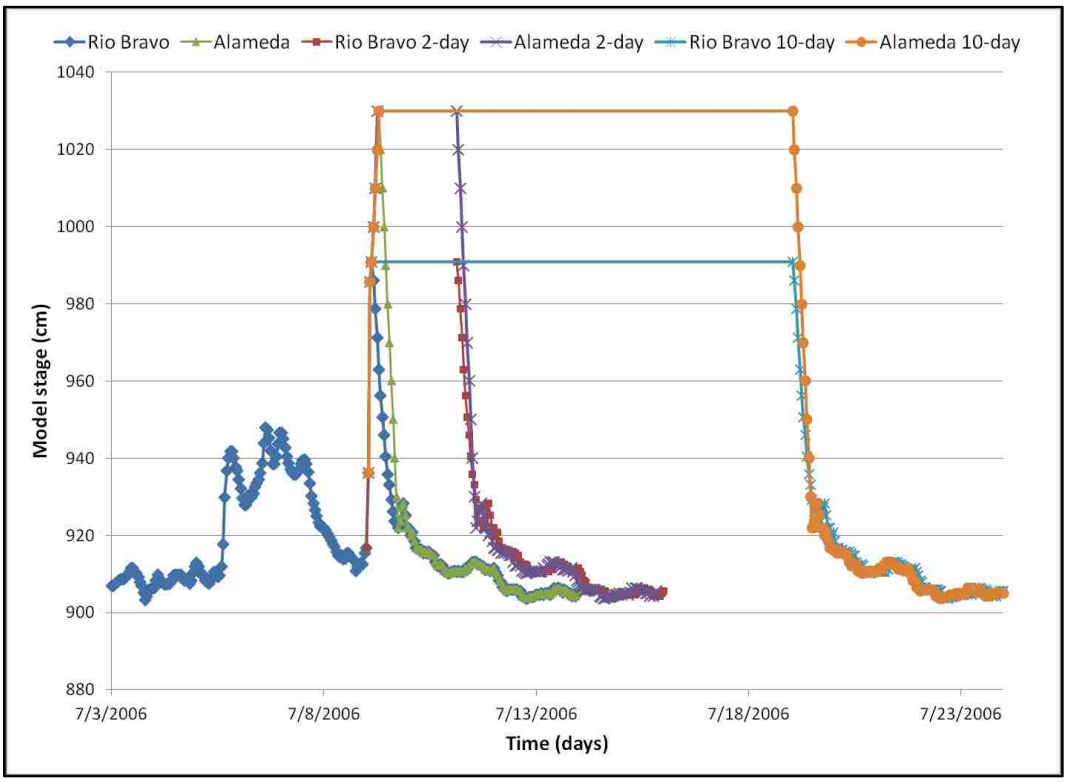

Figure 8. Hydrographs for the 4 scenarios used to study bank storage

peak. These are represented by the Alameda floods shown in Table 3. For the temporal component, considering the historical nature of the Rio Grande included flood events that inundated the floodplain for weeks and even months at a time, while also taking into account the highly engineered river system that exists today, a 2-day and a 10-day

www.manaraa.com

flooding of the lower floodplain were used to study bank storage. The hydrographs for the six model runs summarized in Table 3 and illustrated in Figure 7 were analyzed to quantify the spatial and temporal aspects of bank storage at this location.

Table 4 details the changes that were made to the Rio Bravo baseline model to study the influence of the observed alluvial architecture on bank storage. These included a scenario where the hydraulic conductivity of the lowest layer of low permeability was given the same values as the underlying sandy layer. Also included in this comparison were two scenarios where the entire system was assumed to be homogeneous. One scenario was given the hydraulic conductivity of layer 6 (0.017cm/s) and the second scenario was given a value suggested by Engdahl (2010b) for homogenous analyses completed at this location (3.9m/d = 0.0045cm/s).

Table 4. Model alterations for the scenarios that studied the influence of the stratigraphy on bank storage

Event	Modification
Rio Bravo	Baseline scenario using stratigraphy observed in field.
No low permeability 5th layer	The low permeability layer directly above the base sandy layer was removed. This represents layer 3 of the lower floodplain and layer 5 of the upper floodplain
Homogeneous	No stratigraphy was used and the domain was given a hydraulic conductivity equal to layer 6 (K=0.017 cm/s)
Engdahl (2010b) homogeneous	No stratigraphy was used and the domain was given a hydraulic conductivity equal to what Engdahl (2010b) suggested for groundwater studies at this site (K=0.0045 cm/s)

Results

In order to address the research questions, a mass balance and a flux rate was analyzed for each of the layers as well as for the total profile. Figure 9 shows the integrated flux for the entire system for each of the model runs. Positive flux values represent water entering the system, whereas negative fluxes represent the opposite. Figure 10 shows the

www.manaraa.com

bank storage in the system focusing on the initially unsaturated layers of the model (layers 1-6). A choice was made to include these layers because the storage for the underlying saturated layer remained constant throughout the entire model and was much larger in magnitude due to the thickness of the model. Therefore it would be misleading to include this layer because the storage represented the constant flux of water from the river to the drain and was not the result of a flood event.

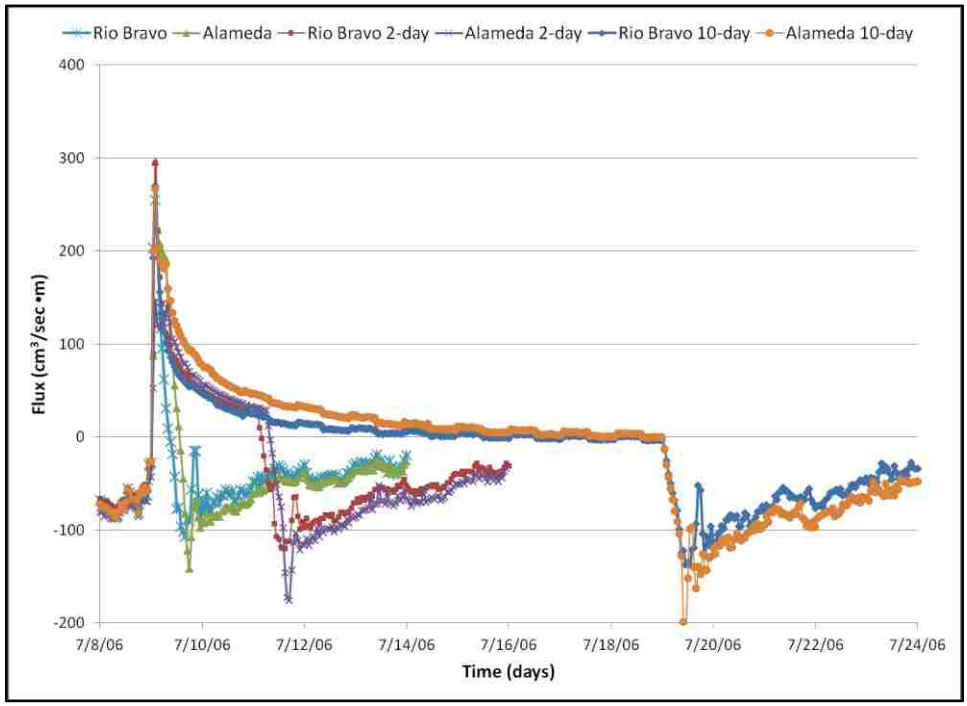

Figure 9. Total flux through the system under all 6 flooding scenarios

Figure 9 and 10 illustrate the flux and storage relationship between the Rio Bravo flood (lowhead) and the Alameda flood (high-head) for each of the time periods. Each scenario experienced a net flux into the vadose zone for the duration of the flood, which was followed by a rapid outward flux immediately upon the flood's recession. Increasing the river stage by 30cm had a minor influence on the flux and storage for the short duration

www.manaraa.com

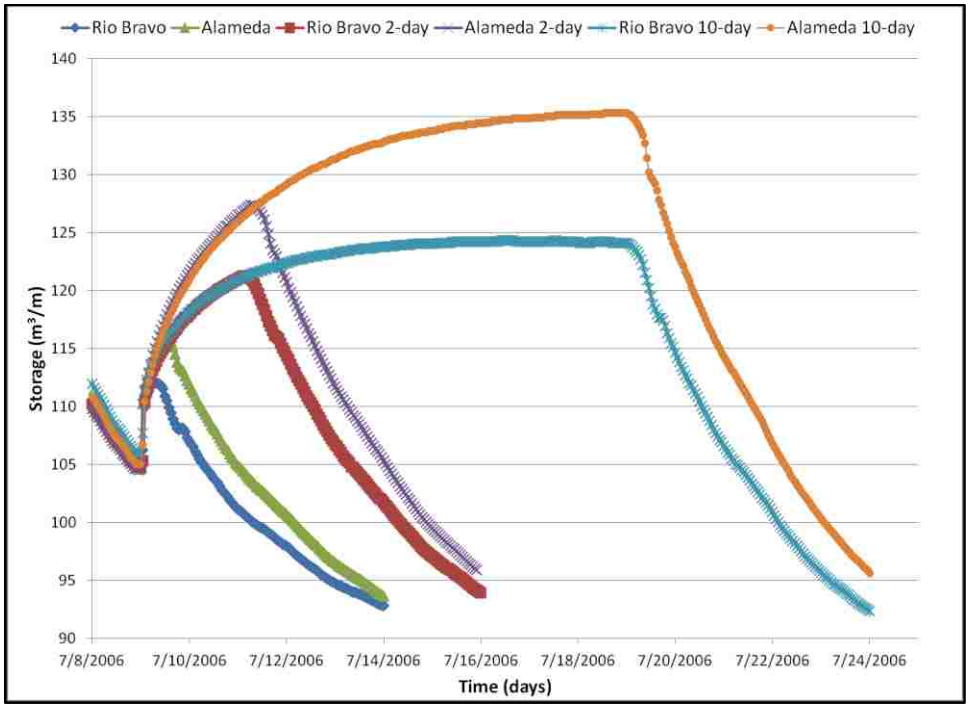

Figure 10. Storage for subregions (layers) 1-6 for each model run

floods, but had a noticeable impact on the 2-day and 10-day flood events. Given that the Alameda flood resulted in greater bank storage for each scenario, the outflow flux is also greater due to the larger hydraulic gradient present at the time of flood recession. Figure 10 also shows that the maximum storage was reached much earlier for the Rio Bravo 10-day flood, whereas at first glance the Alameda 10-day flood storage appears to be increasing at the time of flood recession.

Figure 11 and 12 show the system flux and bank storage for the alternate stratigraphy scenarios. These demonstrate that for the Rio Bravo flood, taking away the low impermeability 5th layer had a minor impact on the flux through the system. This also holds true for the flux through the system when the entire model was given the conductivity of the underlying sand layer (K = 0.017 cm/s). A decrease in conductivity of more than an order of magnitude (from 0.017 cm/s to 0.0045 cm/s) had a substantial

www.manaraa.com

impact on the flux, as evidenced in Figure 11. Figure 12 illustrates the influences these changes have on bank storage. The initial water contents for the two homogenous

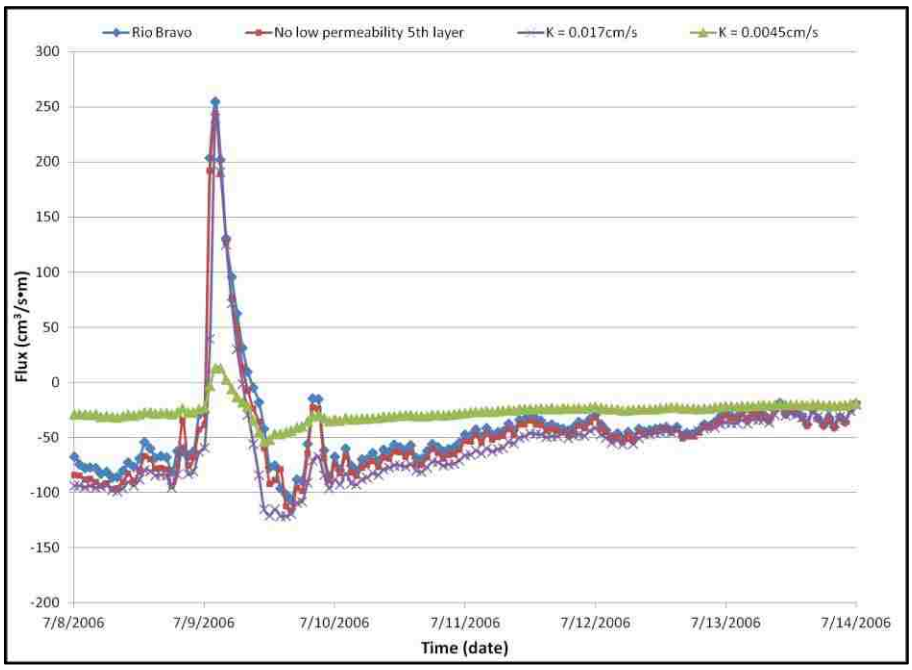

Figure 11. Flux through the system for the alternative stratigraphies

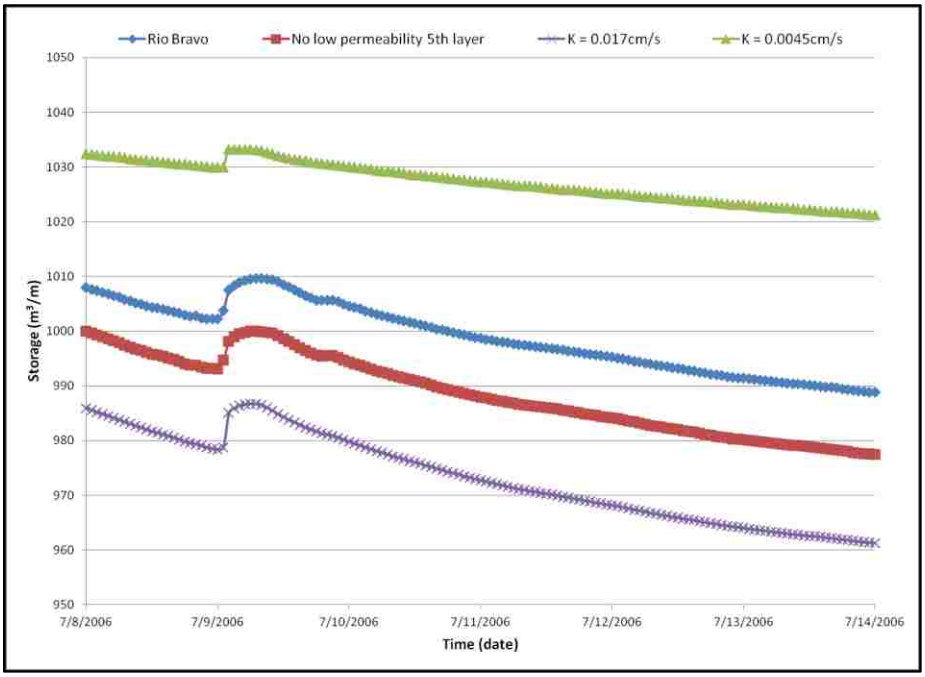

Figure 12. Storage in the system for the alternative stratigraphies

www.manaraa.com

scenarios are much different due to the antecedent impacts of the prior watering of the soil. This shows not only the importance of hydraulic conductivity on the movement of water, but also on the storage of water after a flood event. As discussed above, Figure 8 shows the hydrographs used for this study. A minor pulse entered the system prior to the flood of focus, which resulted in water already being in storage. This also helps to explain why the storage in Figure 10 and 12 is continuing to decrease after the storage water for this flood was released.

Table 5 summarizes the results for the six primary flooding scenarios. The flux and storage values are given on a per meter basis in the streamwise direction, and all times are relative to the beginning of the flood event (7/9/06 @ 12:00 AM).

Table 5. Summary of bank storage capacity and associated times

Event	Time to saturation (hr)	Maximum flux ($cm^3/s \cdot m$)	Volume of water stored (m^3/m)	Time to release (hr)
Rio Bravo	7	254.5	7.5	33
Alameda	12	295.7	11.5	50
Rio Bravo 2-day	50	294.2	16.5	105
Alameda 2-day	54	293.1	22.7	121
Rio Bravo 10-day	178	270.3	19.3	290
Alameda 10-day	219	266.9	31.3	324

From Table 5, along with Figure 10, it can be seen that the three Rio Bravo (low-head) flood scenarios resulted in a considerably lower amount of storage and time to release when compared to the Alameda (high-head) scenarios. This finding is explained by the extra 30 cm of flood stage differentiating the scenarios. The elevated head resulted in an additional 17 hrs, 16 hrs, and 34 hrs of bank storage water residence time for the baseline, 2-day and 10-day floods respectively. During this time, the maximum flux and storage into the upper floodplain layers increased as shown in Table 5.

www.manaraa.com

Table 6. Flux ($cm^3/s•m$) and change in storage (m^3/m) for each flood for the layers in the upper floodplain

	Layer 1		Layer 2		Layer 3		Layer 4		Layer 5		Layer 6	
Event	Flux	Storage	Flux	Storage	Flux	Storage	Flux	Storage	Flux	Storage	Flux	Storage
Rio Bravo	2.09	0.090	6.85	0.116	1.44	0.026	1.96	0.110	12.75	0.091	235.43	6.015
Alameda	2.12	0.114	11.10	0.306	2.91	0.071	9.82	0.169	13.01	0.238	282.82	9.287
Rio Bravo 2-day	2.11	0.092	6.51	0.177	1.53	0.058	1.72	0.130	13.77	0.265	280.45	14.396
Alameda 2-day	2.11	0.114	11.25	0.750	3.41	0.393	9.83	0.937	10.99	0.457	279.60	19.058
Rio Bravo 10-day	2.09	0.090	6.81	0.158	1.56	0.062	1.94	0.121	12.85	0.230	250.88	18.232
Alameday 10-day	2.11	0.114	10.94	1.285	3.50	0.548	10.06	1.249	12.84	0.509	247.36	25.770

All of the layers responded to the 30 cm of additional head with an increase in storage, with layers 2, 3 and 4 showing the greatest increase in storage with an average of 130%, 500%, and 800% respectively. Under the 10-day flood event the system reached a steady state where the flux approached 0 cm^3/s (excluding the atmospheric flux from the surface layer), and the bank storage water had reached a maximum value that persisted for multiple time steps. In the case of the Rio Bravo 10-day flood, the maximum storage was reached at 6.5 days, whereas the Alameda 10-day flood reached maximum storage at 9.5 days. These additional three days to saturation primarily represents the amount of time necessary for the storage in the upper floodplain layers to be maximized. For the observed baseline flood there was an increase of 4 m^3 storage per meter of aquifer. Extending the flood period to two days increased bank storage by greater than a factor of two to 16.5 m^3 of storage per meter of aquifer. A comparison of Table 5 and 6 reveals that the majority of bank storage for all 6 scenarios takes place in layer 6. Layer 6 is shared between the upper and lower floodplains and accounts for no less than 80% of the storage, and up to 94% for the Rio Bravo 10-day event. A detailed description of the individual subregions' responses to the floods, including time to saturation and recession, can be found in Appendix F.

www.manaraa.com

Discussion

The purpose of this research was to: 1) determine the time to saturation (maximum storage) and time to release of water as the result of the flood pulses (described above) that overbanked on the lower floodplain, 2) to understand how the sediment layers observed in the field impact the movement of water in the floodplain, and 3) to understand how river engineering has influenced the hydraulic processes of water movement in the alluvial floodplain being studied.

A finding that was not expected is the time to release of the bank storage water. Previous studies concluded that this process can support baseflows for a considerable time period upon flood recession with documented bank storage water residence times in the realm of 10-times the flood period (Cooper and Rorabaugh, 1963) to 5-weeks after flood recession (Squillace, 1996). However, these studies took place in systems with expansive floodplains (1km Bates et al., 2000; 2500m Chen et al., 2006; semi-infinite Barlow et al., 2000), and some even considered the floodplain to be bounded with a no flow boundary to simplify the mathematics (Pinder and Sauer, 1968; Li et al., 2008). In the case of the highly engineered Middle Rio Grande river system, a intentional hydraulic gradient exists between the river and the river side drains (as described above), to intercept water movement away from the river in order to lower the water table for agriculture and urban development. Consequently, water introduced into the aquifer by the river will be removed quickly by the drains and transported downstream where the water can safely reenter the river.

Another important aspect of this interaction is that the drain system is not directly responsive to increases in stream stage because the drain originates off channel. All the

www.manaraa.com

water that enters the drain is the result of river seepage or irrigation returns from the east side of the river. Observed data supports this relationship, and therefore the increased hydraulic gradients results in a proportionally increased flux to the drain. This process was evident in the model results (Appendix F includes a detailed description and images of the results), as velocity vectors illustrated this movement throughout the entire model run. An analysis of the fluxes through the boundaries indicates that nearly all of water that entered the system through the river boundary exited through the drain boundary. This explains why the bank storage water had such a short residence time in the 270m floodplain, as detailed in table 3. Even in the Alameda 10-day scenario which recorded the largest amount of storage, the entire volume was discharged within 3.5 days (84 hrs) upon the floods recession.

The alternate scenarios depicted in Figure 11 and 12 shows the impact of the layering as well as the sensitivity of bank storage to variations in hydraulic conductivity. When the bottom low permeability layer was replaced with a conductivity layer equivalent to layer 6, the storage in the entire system decreased by 10 m^3/m. As would be expected, the majority of this lost storage was from the fourth and fifth layers. The fourth layer, which is predominantly sand, decreased in total storage from ~13.5 m^3/m to 8.5 m^3/m. The fifth layer, which contained a significant portion of fines (38.3%), decreased from ~6.8 m^3/m to ~1.9 m^3/m. Layer 3 also showed a decrease in storage of ~1 m^3/m as a result of the flood and this is most likely due to the drier conditions in the layers below. Layer 6 showed a small increase in storage as a result of the alteration of layer 5, and this reiterates the drainage factor that added complexity to determining the initial conditions of the model.

www.manaraa.com

The next scenarios were homogeneous model runs that cleared the entire floodplain of the observed layers. Multiple scenarios were run with hydraulic conductivities that ranged orders of magnitude. Figure 11 and 12 include two of these scenarios. The first of which extended the change made to the fifth layer, described above, to the entire system. The results of this change exacerbated the drainage and decreased aquifer storage by 23 m^3/m. The influx from the flood wave showed a 1 m^3/m peak increase above the baseline case which added 7.5 m^3/m; however this water drained quicker as can be seen by the slightly increased slope in the recession portion of the curve for the homogeneous run.

The second homogeneous scenario included in Figure 11 and 12 utilized the hydraulic conductivity proposed by Engdahl (2010b) for studies at this site. As can be seen by these figures this conductivity did not model the shallow aquifer very well. The flux in figure 10 is highly dampened compared to the other scenarios, and this emphasizes the sensitivity of the system to a change in conductivity. Given that bank storage, and water movement in general, at this cross section is dominated by flow in the highly conductive sandy layers, a change to these values had a significant change in the system's response to the flood. As a result, bank storage was practically muted to a value that was half of the baseline scenario. This agrees with previous researchers that have emphasized the sensitivity of bank storage to floodplain hydraulic conductivity (Squillace, 1996; Hantush, 2002), with lower conductivity aquifers storing much less than aquifers with higher conductivities (Chen et al., 2006). Engdahl's study focused on the bulk movement of water in the saturated portion of the aquifer over a much larger 3-dimensional area that incorporated a wider range of sediment types and an aquifer depth 3-times what was modeled in this study. Therefore, the impact of low permeability layers (potential

www.manaraa.com

aquitards) underlying the unsaturated layers that dominated bank storage potentially disrupts the ease of water movement experienced at the water table. Also, Engdahl cautioned against the use of homogenous conductivities due to the high degree of heterogeneity at the site, and only proposed the homogenous values for users conducting small-scale studies within a close proximity to the study area.

Conclusion

Two previous studies collected data on this system, and the results from the current research built on this knowledge by contributing insight into the impact the observed stratigraphy has on bank storage, along with the temporal and spatial components of this phenomenon. These results indicate the importance that the alluvial architecture of the floodplain plays in storing water in the shallow aquifer. Without the low permeability layers of silts and clays near the surface the floodplain systems capacity to hold onto water decreased. Although the system mimicked the magnitude of the flood peak, the total storage was considerably less and the drainage rate increased as a result. The layering of the system potentially plays an important role for the biotic community. Given that considerable roots were found in the low permeability layers, means that these layers provide a supply of necessary water and nutrients to the flora. As is known, a healthy autotrophic community provide the foundation for the health of the rest of the ecosystem.

The results also showed how the highly engineered Rio Grande's capacity to store water during a flood event to support baseflows for prolonged time periods is impeded due to the drainage system. Bank storage water was transported out of the floodplain in 1-day for the baseline flood, and only 3-days for the Alameda 10-day extended flood due to the

www.manaraa.com

anthropogenic hydraulic gradient. The additional 24m^3/m of water that was stored by the latter flood, helped to support flows in the drain for 2 days past the baseline case. A flux to the river only occurred immediately following the recession of the flood and included an insignificant amount of water. The predominant flux was in the direction of the drain and accounted for the majority of water that entered the system. The flux through the base of the model accounted for less than 1% of the influx from the river.

River management practices of the Rio Grande have produced a system that has degraded the important ecosystem service of bank storage. Human activity around the river, especially agriculture, urbanization and alteration of the flooding process as a means of controlling and/or storing water, interrupts the natural processes and thus disturbs the functions and overall health of the ecosystem (ASFM, 2008). As a result, an environment has been created that allows for invasive species to flourish while native species are in decline. Overbank floods and floodplain inundation, which used to provide important services, have not occurred on a major scale in the Middle Rio Grande for over 70 years. Research has shown that a minimum annual deposit of 0.5 cm will inhibit floodplain pedogenesis (Daniels, 2003), and others have found that the lack of disturbance can result in the development of a hydrophobic surface layer due to the build-up of hydrocarbons (Molles et al., 1998). Although these processes may not considerably impact bank storage at this site because the lower floodplain periodically receives floodwaters and storage was shown to be dominated by the horizontal movement of water, it is predicted that they will influence the response of the system to precipitation events. Combined with the accumulation of a thick coarse particulate organic matter layer on the surface

www.manaraa.com

composed primarily of leaves, sheet flow may occur that transports water directly to the river, thus negating important floodplain services..

Further research investigating the infiltration capacity of the surface soils will help to provide a accurate depiction of how the system responds to floods, as well as the impact of soil formation processes on the hydraulic conductivity of floodplaina . Also, developing a model with a much wider floodplain without the inclusion of a drain can offer insight into the historical bank storage capacity. Future research should also include aspects of hysteresis and root water uptake. For this study root water uptake was left out because the transpiration component was not thought to play an important role due to the short duration of the model run. However, research has shown that roots can impact the hydraulic conductivity of the soil. This additional complex variable has a wide range of implications for conductivity, and needs to be investigated further to understand its impact on bank storage. Hysteresis, although thought to play an important role in bank storage due to the wetting and drying of the soil, was left out due to the increased non-linearity to the model, and also because of a lack of data to describe the process with confidence. The water retention curves used to obtain the soil parameters were drying curves, and wetting curves would have resulted in parameters that exhibited lower conductivities at the same pressure head.

www.manaraa.com

Appendix A- History of site

Historically, the indigenous communities in the area have been irrigating extensively in the area for hundreds of years. The Isleta culture, whose name translates to "island", constructed their pueblo on raised land to avoid the repercussions of flood water which would come rushing down the San Juan Mountains on a regular basis (Molles et al., 1998). As waters flooded the settlers in the area and displaced many residents, the Isleta pueblo remained intact due to their location. Out of these devastating floods, came the need/desire to control the river to prevent flooding while increasing the amount of land that can be farmed and later urbanized. A timeline of the major floods and response through the development of infrastructure is included in figure 12.

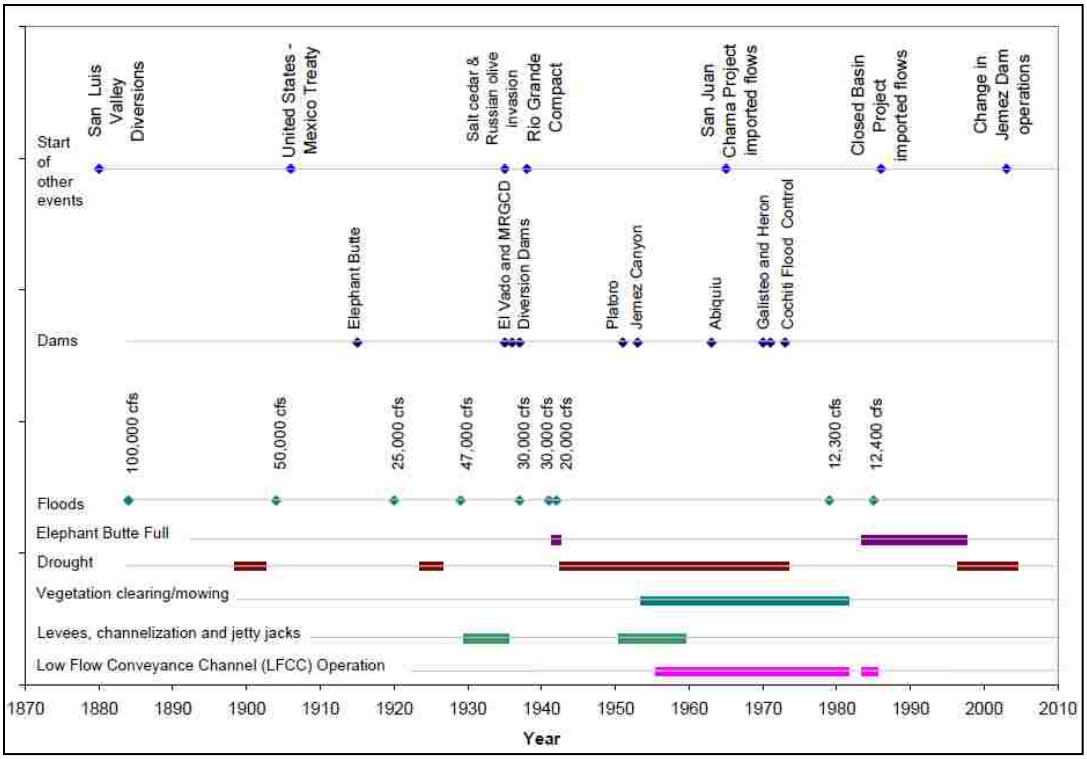

Figure 13. A timeline of flood events, dam construction and other important events for the MRG (Makar et al., 2006)

www.manaraa.com

The Middle Rio Grande Conservancy District was created in 1923 to "provide flood protection from the Rio Grande, and make the surrounding area hospitable for urbanization and agriculture" (MRGCD website). The works that followed eventually successfully drained the land and managed to control the once mighty river. By the year 1935, the MRGCD had built the El Vado storage dam, as well as multiple diversions. In total they dug 817 miles of new canals, added 200 miles of riverside levees, added a system of jetty-jacks, and constructed a series of drains that funneled water away from the river while lowering the water table to dry out the land (MRGCD website). Figure 13 is a 1935 image of the Rio Bravo section of the river prior to the construction of the Rio Bravo Bridge.

Figure 14. An image of the Rio Bravo reach of the Rio Grande taken by the MRGCD in 1935

Figure 13 includes the drains that were constructed as well as the anthropogenic channel which later became the lower floodplain in the model. Due to major flooding in 1941 and

www.manaraa.com

1942, the MRGCD enlisted the help of the federal government to build larger flood control structures upstream. As a result the Bureau of Reclamation and the Army Corp of Engineers spent over $70 million dollars building new flood control reservoirs while also rehabilitating and modernizing MRGCD facilities (MRGCD website). Figure 14 is an image of the same area in 1953 showing the change in the river after the major floods of 1941 and 1942. The main difference between these images is the channel that was cut through the area is no longer isolated from the rest of the riverbed. There also appears to be a large amount of sedimentation and vegetative growth in areas that were flooded 12 years previous.

By this time the major upstream dams built to control flooding and sedimentation were either just coming on-line (Jemez Canyon Dam) or had not been built (Abiqui Dam, Galiseo Dam, Heron Dam, and Cochiti Dam). Figure 15 is a 1973 image of the same area showing the impacts on the Rio Bravo reach of the Rio Grande from the upstream infrastructure, as well as the construction of the Rio Bravo Bridge just downstream of the site. The 1973 image shows how the river has substantially decreased in width at the site with pinch points near the middle and bottom of the image. The lower floodplain has clearly begun development, and a significant amount of vegetation has taken root all along the eastern side of the river.

www.manaraa.com

Figure 15. A 1953 image of the Rio Bravo reach

Figure 16. A 1973 image of the Rio Bravo reach including the bridge

www.manaraa.com

Appendix B- Field work

Four locations along the Rio Bravo cross section were chosen for this study. Site 1 was directly next to the river bank. Figures 16 through 19 show site 1 and the hole that was excavated to obtain the sediment samples.

Figure 17. A view of site 1 as it is approached from the brush

Figure 18. The exposed hole that was used to obtain the samples from site 1

www.manaraa.com

Figure 19. The lithology of site 1 with alternating layers of fine and coarse sediments

Figure 20. A core sample taken from layer 2 composed primarily of sand

www.manaraa.com

Site 2 was located at the base of the slope dividing the upper and lower floodplains. The top soil layer was covered with an 8inch think layer of organic debris, primarily bark, interstitially filled in with a dark soil type. This layer was impossible to obtain a core of for laboratory analysis, and thus was left out of the description used for the model. Figure 20 shows evidence of a similar layer on the upper floodplain with the densely vegetated lower floodplain shown in the distance.

Figure 21. The landcover on the upper floodplain with the highly vegetated lower floodplain in the distance

At first, this layer was not as apparent on the lower floodplain. It was only after the shovel entered the soil, and difficulty was encountered that the layer was exposed. Figure 21 shows the bark that had accumulated on the surface since the last major flooding, and has since been secured by roots and overlain sediments.

www.manaraa.com

Figure 22. The large woody debris that lay directly under the surface, and was exposed at site 2

Figure 22 shows the undisturbed surface layer at site 2 as well as the slope up to the upper floodplain that remains as a result of the anthropogenic channel detailed in Appendix A.

Figure 23. The surface of site 2 along with the slope up to the upper floodplain

www.manaraa.com

Figure 23 shows the exposed water table. The alternating layers of sediment cannot be seen easily in this image due to the root system. Figure 24 is a close-up of the top foot of layering of site 2. The surface layer dominated by organics is underlain by a clayey layer around the 1.5'-1.7' mark.

Figure 24. The exposed water table at site 2 along with the dense root structure that made digging the hole difficult

Figure 25 shows the location of site 3, which was excavated on a functioning road. This was the first site to be uncovered, and the soil conditions were extremely dry. The work took place immediately following the reopening of this park by the city of Albuquerque. The park was closed because of high fire danger and more than 100 days without rain. On top of that there was no vegetation in the immediate vicinity of the hole as well as a lack of sun cover.

www.manaraa.com

Figure 25. The top foot of layering at site 2

Figure 26. The location of site 3 including the infrequently traveled access road

www.manaraa.com

Figure 26 shows evidence of these dry conditions, as the top surface layer composed of fines is indistinct from the sandy layer below.

Figure 27. The hole that was dug at site 3

Site 4 was located in a much more heavily vegetated area (Figure 27). There were a few large roots (>2in. diameter) that were removed in the process of digging the hole. Also, there was a layer of organic material covering the surface which was primarily composed of leaves. Figure 28 clearly shows the stratigraphy of the hole. The top layer composed of fines at this location is visibly distinct from the underlying layer of sands. This is a result of both the organic layer covering the surface, which limited soil evaporation, as well as a precipitation event that had occurred between the excavation of sites 3 and 4.

www.manaraa.com

Figure 28. The location of site 4

Figure 29. The depth to the water table and the alternating water holding layers present at site 4

www.manaraa.com

Appendix C- Lab work

Laboratory analyses were completed to understand the soils and to determine the hydraulic properties of the samples obtained during field work. These include the particle size distribution, saturated hydraulic conductivity, dry density, specific gravity, and the development of water retention curves. Initially, the number of samples taken was limited by the number of caps for the sample cores. However, after more caps were purchased from a local supplier this was no longer a limiting factor. The dimensions of the samples used in calculations of the hydraulic conductivities were: 15.3 cm in length, with an end area of 29.61cm^2.

A qualitative laboratory analysis was completed on soil samples for the east river and east Bosque wells, obtained from the original USGS cores for the site. The NRCS manual approach was chosen because sample size was limited due to the preservation of the cores for future research.

Included below are pictures of some of the laboratory work that was completed.

Figure 30. Dry samples from site 3

www.manaraa.com

Figure 31. Sample 1, layer 1 specific gravity test with the sieves for the particle size distribution in the back

Figure 32. Caps used for the hydraulic conductivity samples. Screens restricted swelling of sample during saturation

www.manaraa.com

Figure 33. Constant head (right) and falling head (left) hydraulic conductivity apparatus

The main issue encountered with the hydraulic conductivity test was with the sealing of the sample. The basins shown in figure 31 were used after a few of the samples had leaked, which resulted in a significant amount of ponded water on the floor and in the drawers. A silicon gel was used as the sealant, and at the beginning it took 2, 3, or 4 attempts to seal a sample successfully. The samples composed of fine sediments leaked more frequently due to the sustained pressure gradient across the sample. Issues of sediments passing through the 40 micron porous mesh used to cover the samples occurred for the fine samples as well.

www.manaraa.com

Figure 34. Hanging column test apparatus built for this study

www.manaraa.com

Appendix D: Model development

Initially the model was constructed using HYDRUS 1.0, but due to limitations of the software in modeling large gradients over small distances, an upgrade was made to HYDRUS 2.0. The initial conditions of the model were chosen as a gradient from 0.25 to 0.43 from the surface to the water table. This is captured below in Figures 33 and 34, which show the entire domain as well as the top 3 meters of the transition from the lower to the upper floodplain, respectively. Since the initial conditions were unknown for this time period, the model was run for 5 days prior to the flood event to allow for the system to equilibrate, with the assumption that the state that was reached when the flood came through was a close approximation of the actual conditions. However, it is known that this is a large assumption since the soil moisture properties of the system are highly heterogeneous and may well have been incorrectly assumed.

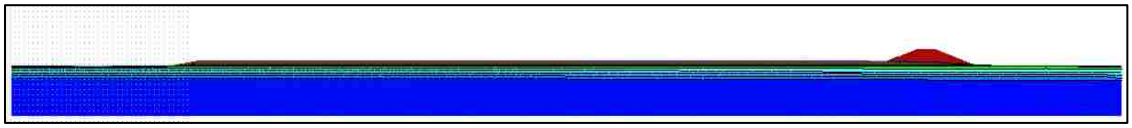

Figure 35. Initial conditions of the model for the entire domain

The boundary conditions for the domain were based upon figure 2. The side boundaries, representing the river and the drain, were Time Variable Head (TVH) boundaries. The hourly data for these was input from the USGS website (http://nm.water.usgs.gov/projects/riograndesections/). The bottom boundary condition was chosen to be a flux boundary. The hourly data for this boundary was calculated using the hydraulic gradients present at the wells, combined with a hydraulic conductivity that

www.manaraa.com

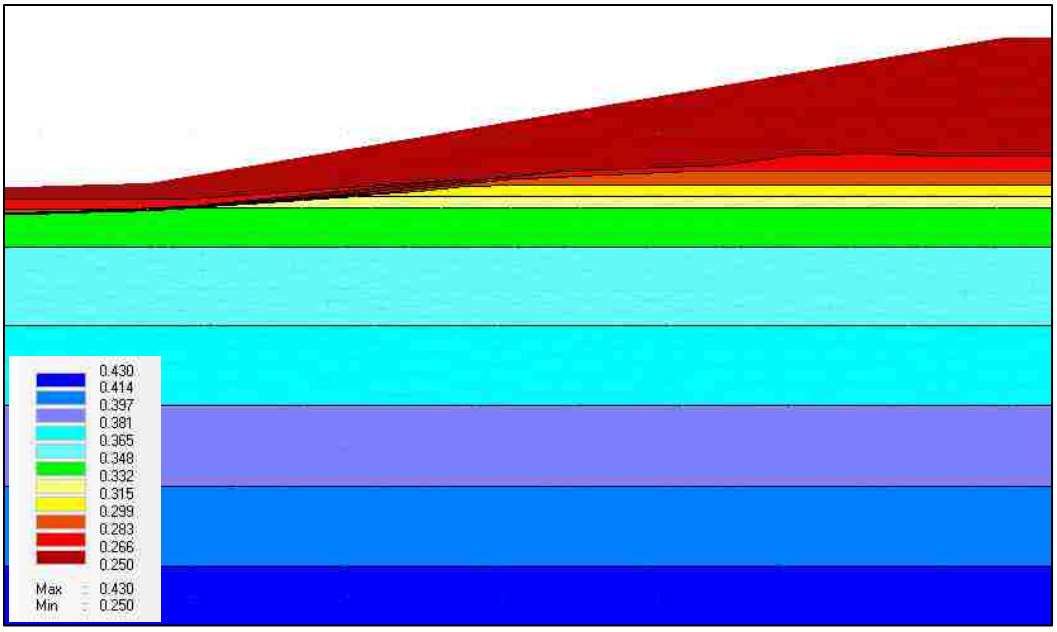

Figure 36. Initial conditions with scale for the top 3 m of the transition zone between the lower and upper floodplains

was determined by slug tests completed at this site by the USGS in a separate study focused on understanding the amount of water lost by the river to the drains in the Albuquerque reach of the Middle Rio Grande (Rankin et al., 2011). The results of this analysis were compared to estimates of the vertical flow of water at this site in a separate USGS study through the use of heat tracers (Bartolino and Niswonger, 1999), and were determined to be a close approximation. Given that the fluxes were within one order of magnitude, and the data used was relative to the actual conditions at the site (dynamic hydraulic gradients), using this approximation of the vertical flux was deemed to be a better characterization of the field conditions.

The FE mesh for the model was composed of 24,843 elements. This portion of the model development was extremely difficult to complete due to the large difference in spatial dimensions between the depth (10 m) and width of the cross section (270 m), along with

www.manaraa.com

the fine layers that were being modeled. The thinnest of these layers were approximately 5 cm, and to model the gradients across these layers more accurately they were broken down into 4 sub-layers, thus resulting in FE layers of 1.25 cm. Figures and show the FE mesh for the entire system and for a close up of the lower floodplain, respectively.

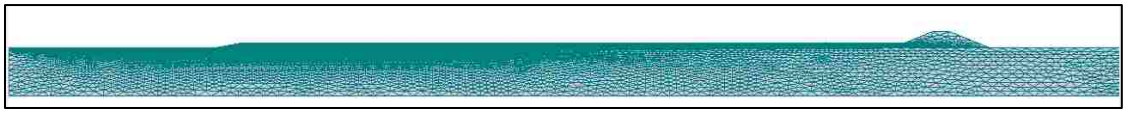

Figure 37. FE mesh for entire domain

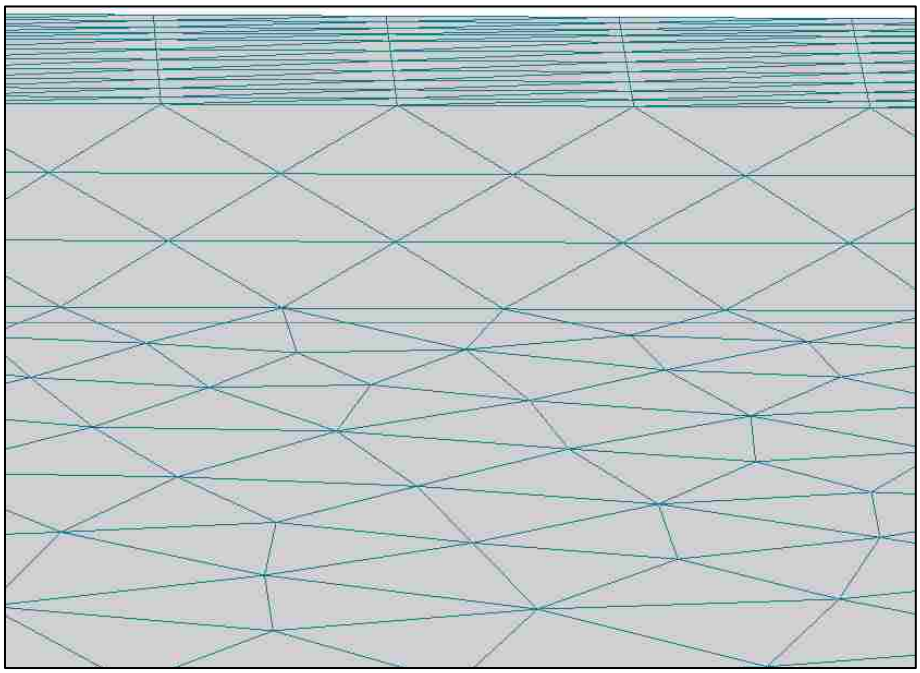

Figure 38. FE mesh for the top 4 layers of the lower floodplain

The lower floodplain is composed of 4 layers and the upper floodplain is composed of 6 layers. The choice was made to give each of these different soil properties associated with what was found in the laboratory (table 1). HYDRUS-2D calculates a mass balance for any subregions in the model, and the choice was made to construct separate subregions for the lower and upper floodplain, as well as for the initially saturated and

www.manaraa.com

unsaturated layers. This allowed the layers that were inundated during the flood to be analyzed separately from those that were not. The subregions for the lower and upper floodplain, along with the underlying saturated layer, are shown below in figures 37 and 38 respectively. The water retention curve parameters (α and n) were given based upon the results shown in figures 59 and 60.

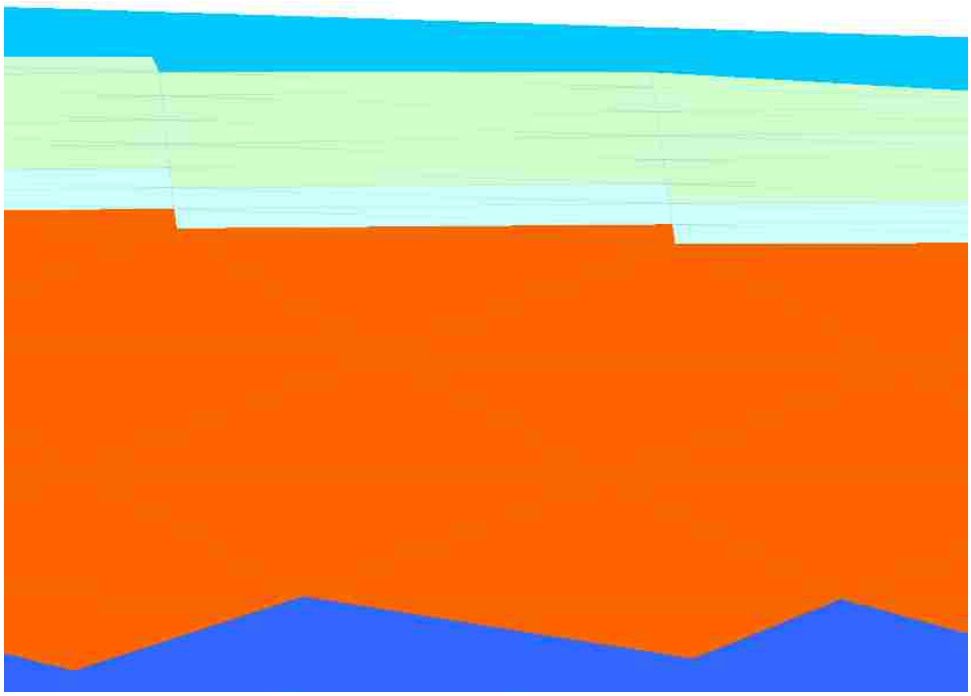

Figure 39. Subregions generated by HYDRUS for the 4 layers of the lower floodplain

To answer the questions posed for this research a total of 9 model runs were chosen. The first 6 focused on understanding the spatial and temporal aspects of bank storage. A baseline flood event, known as the Rio Bravo flood, was run under the recorded conditions in the field. However, since this event was fairly brief in nature, the flood was extended for 2 and 10 days to see how the system would respond to a flood of longer duration. Another extension was made to the baseline event, and that was to increase the

www.manaraa.com

peak flood stage by 30 cm. This flood was named the Alameda flood. This was done for two main reasons. Firstly, when the flood pulse entered the system upstream (at Alameda) it was approximately 30 cm greater in stage, so it was thought that this adjustment was reasonable. Secondly, the additional 30 cm of head increased the number of layers in the upper floodplain, and therefore provided insight into the role the stratigraphy played in bank storage. These 6 floods were used to study the temporal and spatial components of bank storage.

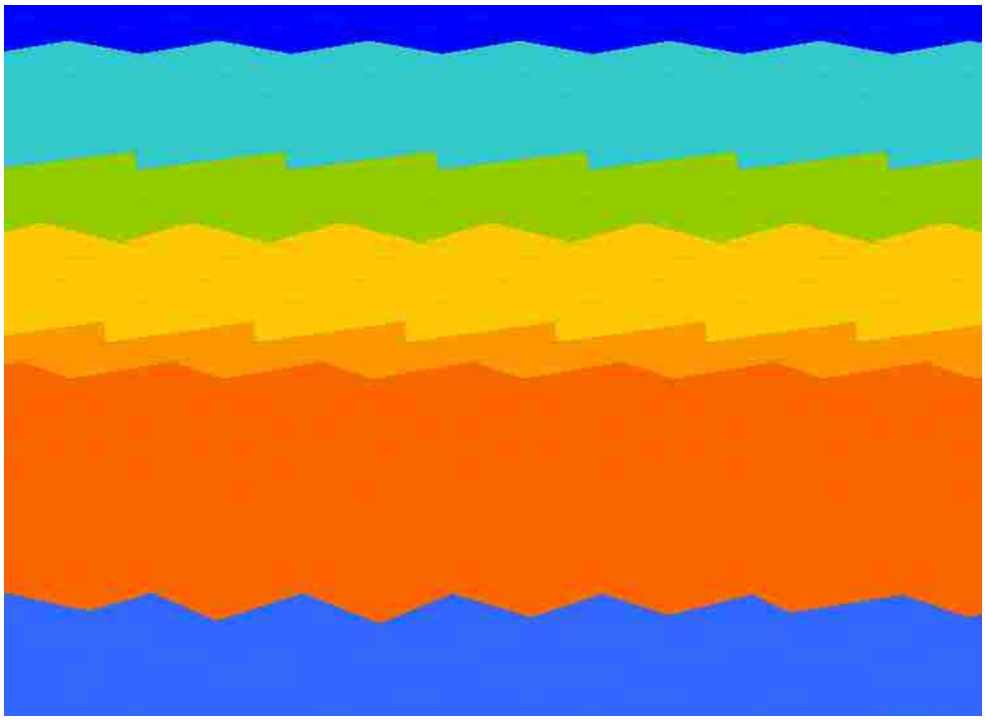

Figure 40. Subregions generated by HYDRUS for the 6 layers of the upper floodplain

The next three scenarios focused on the impacts of the stratigraphy as well as the hydraulic conductivity on bank storage. The first scenario to be described removed the low permeability layer that was directlyabove the sand layer occupied by the water table. This scenario was chosen to see the influence this low permeability layer had on the

www.manaraa.com

rising of the peak, as well as the impact it had on the storage of water in the overlying sandy layer. The next scenario made the entire system homogeneous and was given a hydraulic conductivity of the underlying sandy layer (0.017 cm/s). This value was chosen because it was on the higher range of conductivities. The results from this scenario were going to be compared to the final scenario, which was also homogeneous. This final scenario was given a lower conductivity and was chosen because it was suggested by a researcher who completed a ground water study at this site (Engdahl 2010b). Engdahl's (2010b) study focused on the impacts of heterogeneity on the movement of ground water in this area, and he said that homogenous domain assumptions should not be applied to the system without some understanding of the heterogeneity present. However he did provide an effective hydraulic conductivity to use for homogenous studies that provided comparable results to the stochastic modeling he conducted (Engdahl, 2010b).

www.manaraa.com

Appendix E: Lab results

Below are the particle size distribution curves for all of the layers.

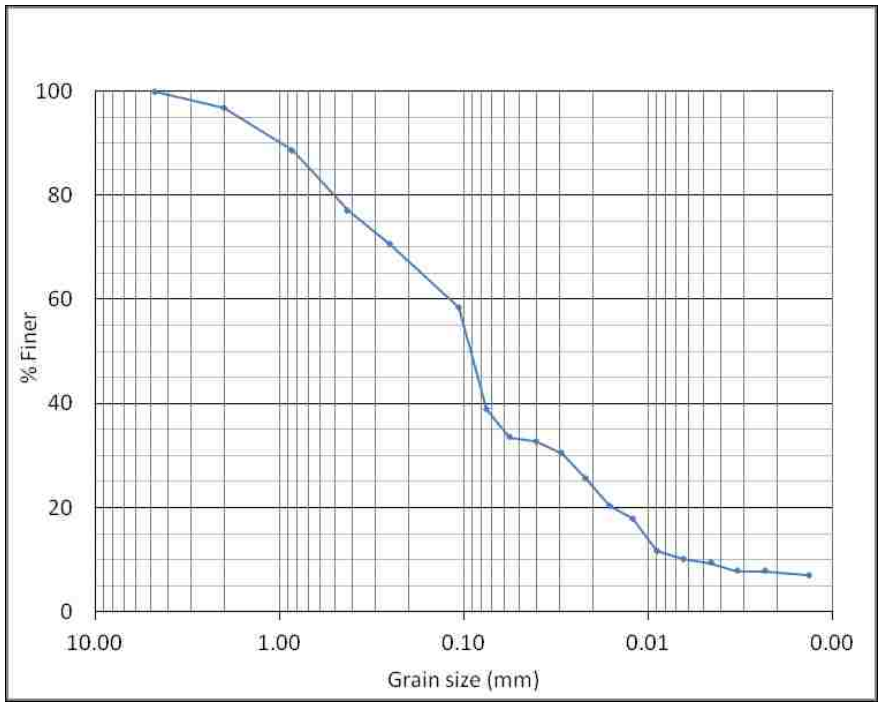

Figure 41. Site 1, layer 1

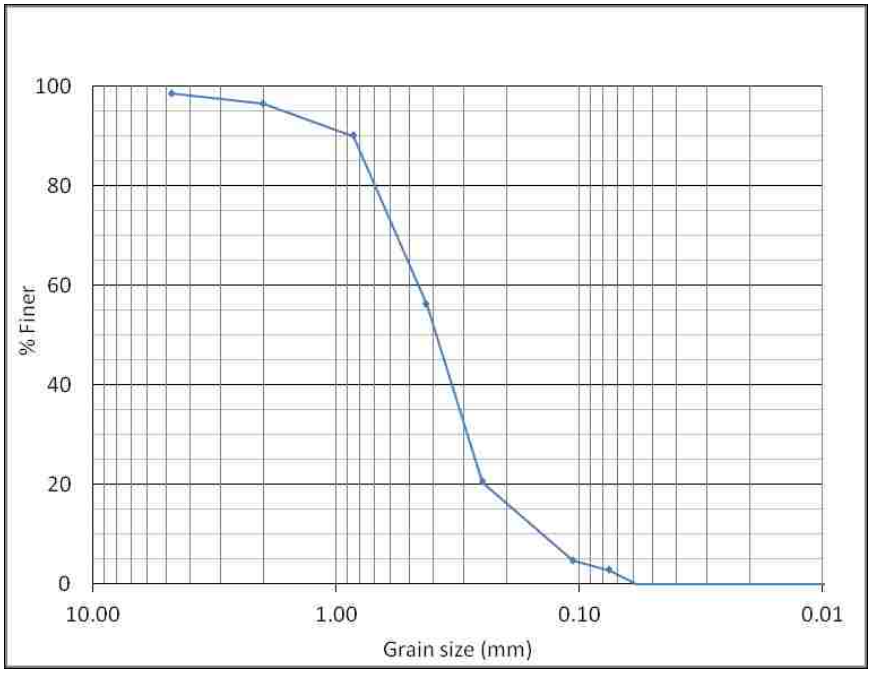

Figure 42. Site 1, layer 2

www.manaraa.com

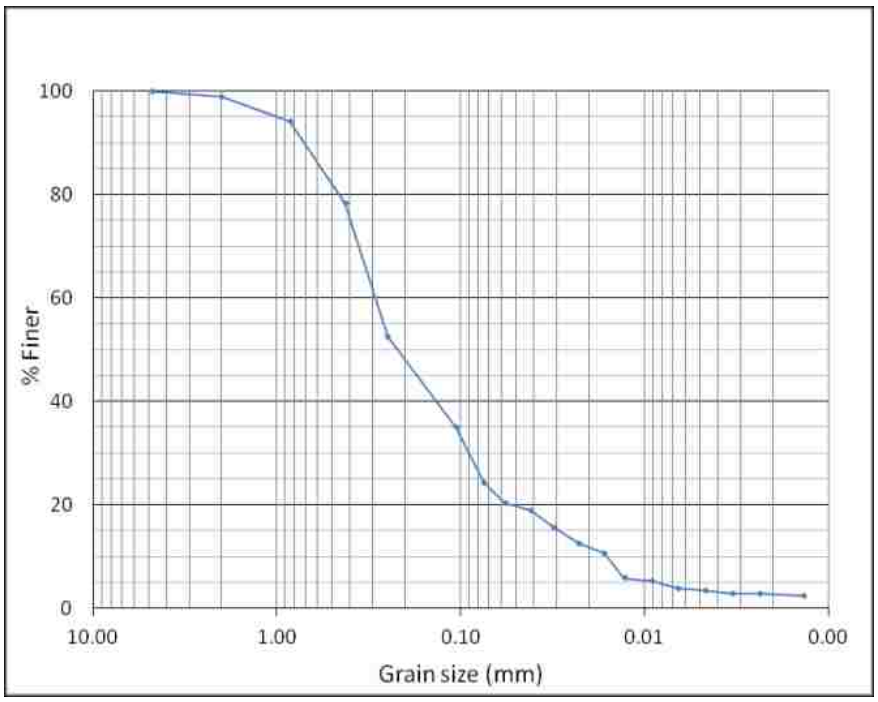

Figure 43. Site 1, layer 3

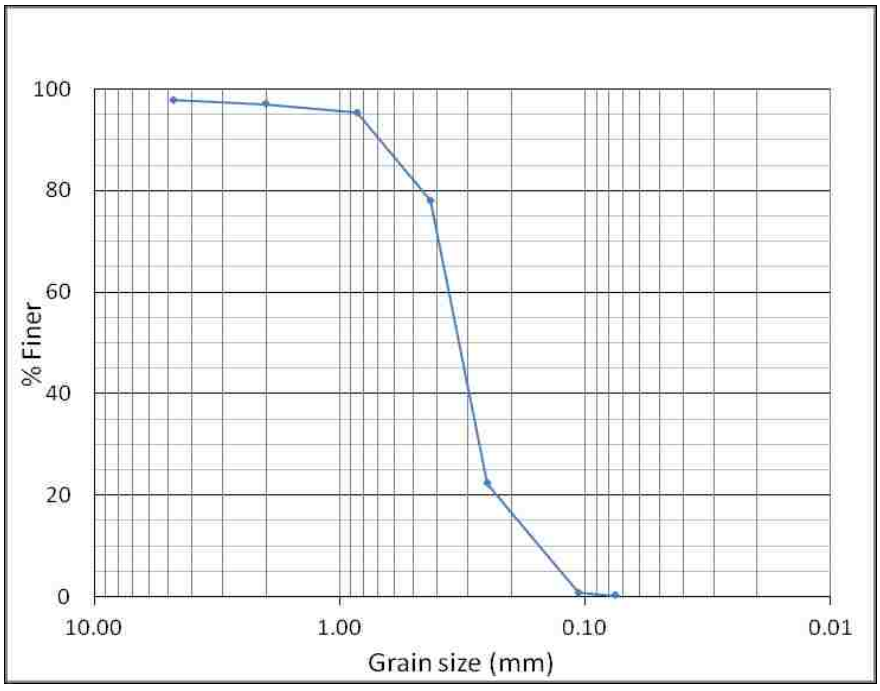

Figure 44. Site 1, layer 4

www.manaraa.com

The alternating layers can be clearly seen by the curves that detail the sediments found at site 1. Layers 1 and 3 have distributions of a well graded soil, where as layers 2 and 4 display the features of poorly graded soils. These index properties offer insight into the hydraulic conductivities that would be expected for each layer. This same pattern continues throughout all of the sites.

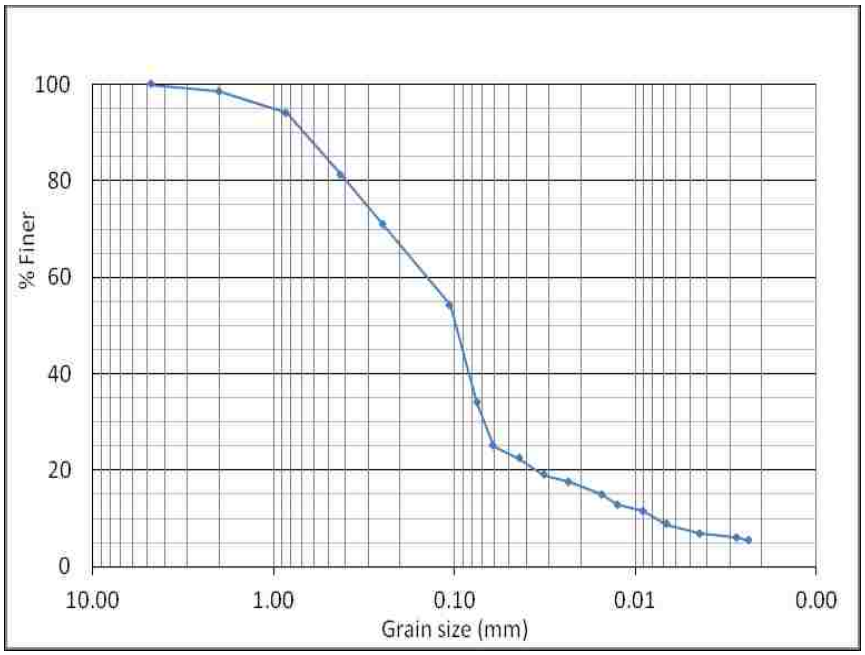

Figure 45. Site 2, layer 1

www.manaraa.com

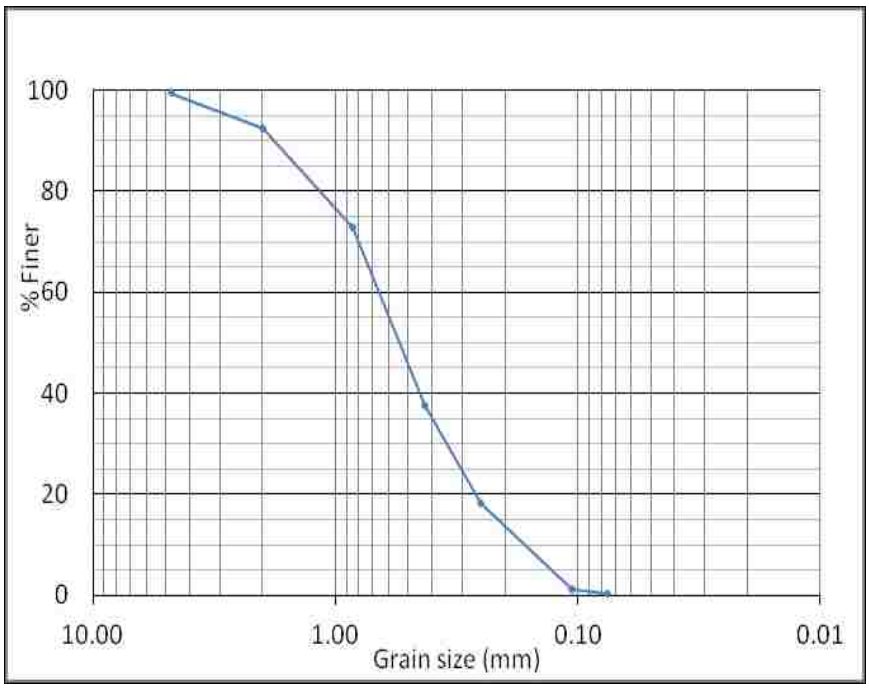

Figure 46. Site 2, layer 2

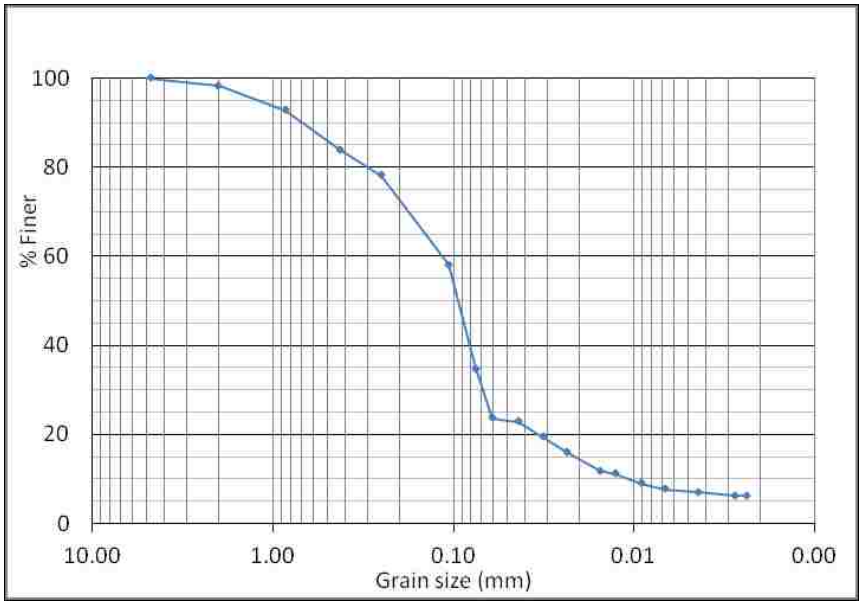

Figure 47. Site 2, layer 3

www.manaraa.com

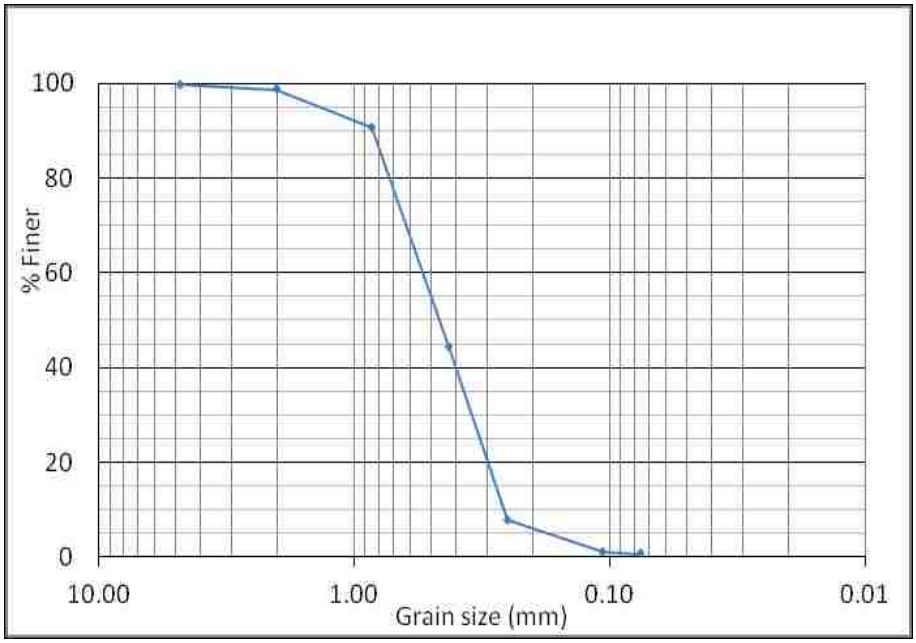

Figure 48. Site 2, layer 4

Site 2 displays the same characteristics as site 1. The 8" organic layer was left out of this analysis, as well as those to follow.

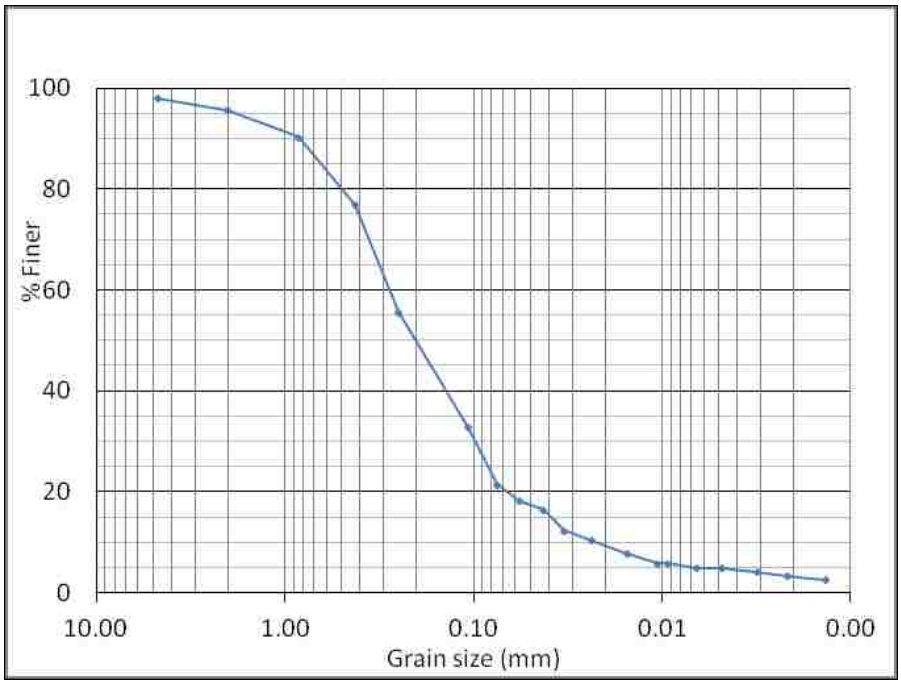

Figure 49. Site 3, layer 1

www.manaraa.com

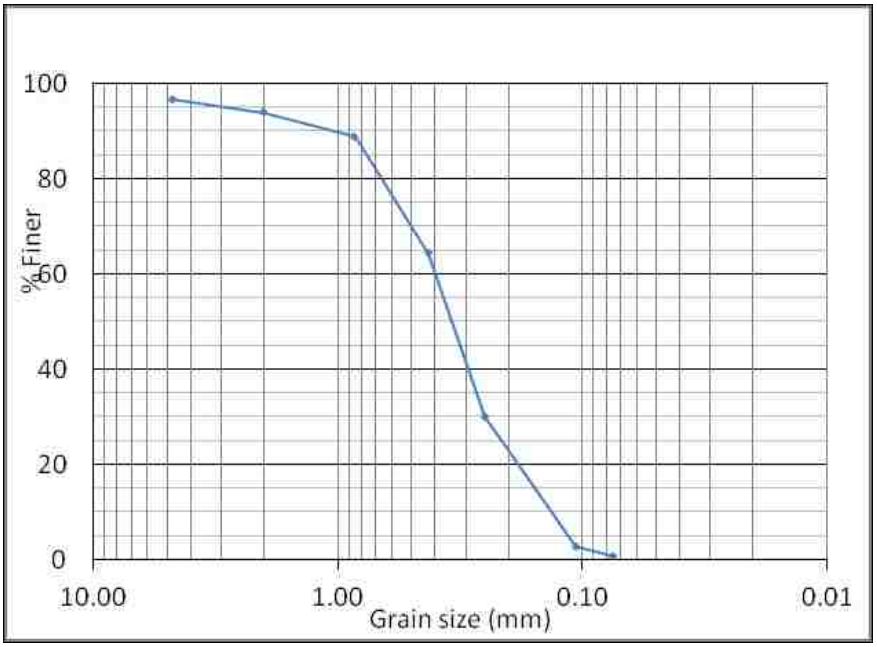

Figure 50. Site 3, layer 2

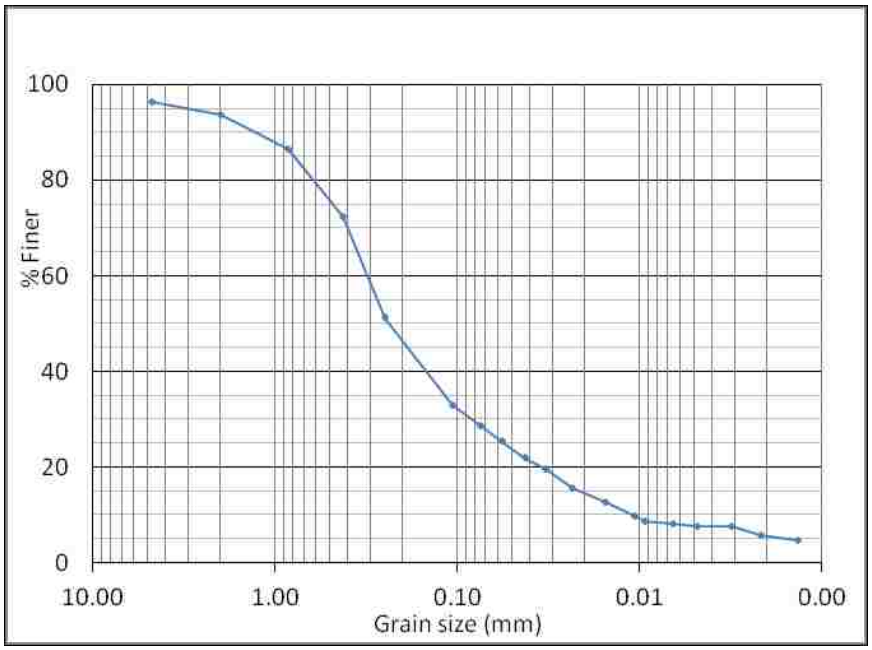

Figure 51. Site 3, layer 3

www.manaraa.com

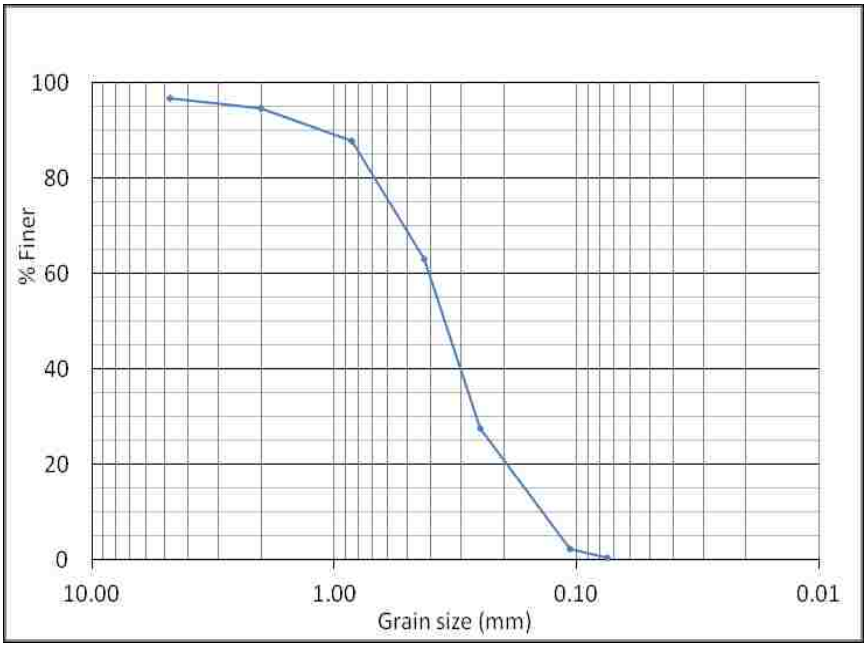

Figure 52. Site 3, layer 4

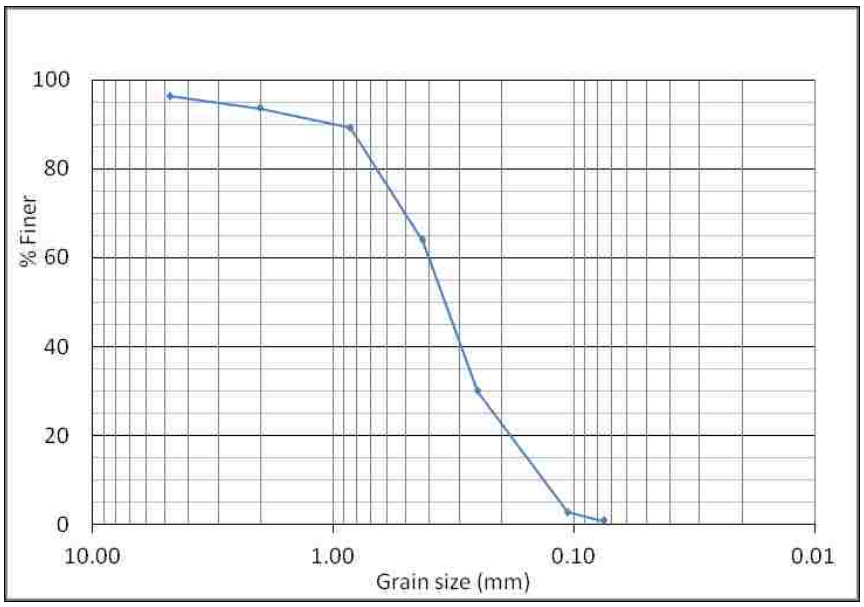

Figure 40: Site 3, layer 6

As mentioned above, site 3 was the first site to be excavated. At this time the field methods were unrefined and the majority of the particle size distribution curves were obtained through the samples taken for the hydraulic conductivity tests. However, since

www.manaraa.com

the sample from layer 5 was lost during the process, which meant that there is also missing data for the particle sizes from this site.

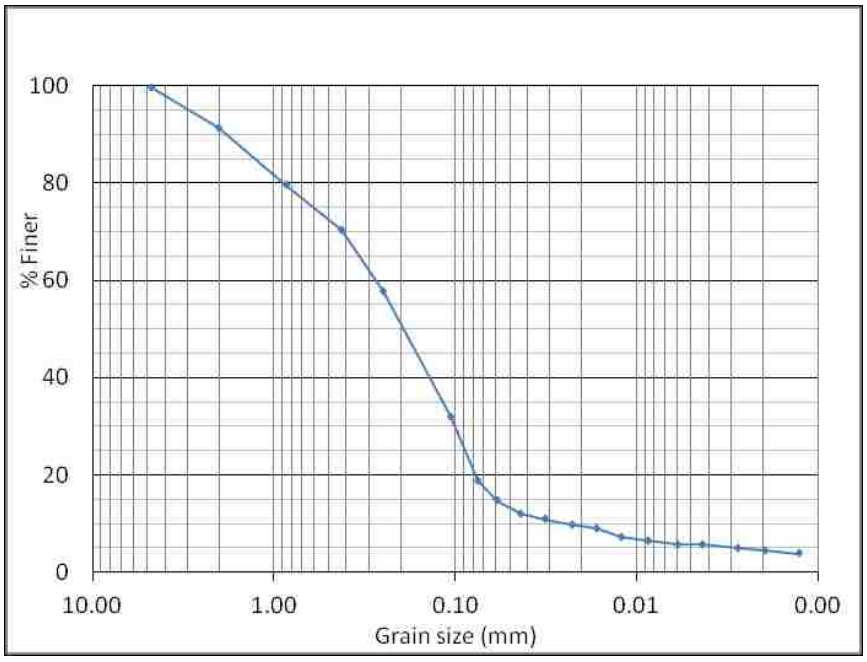

Figure 53. Site 4, layer 1

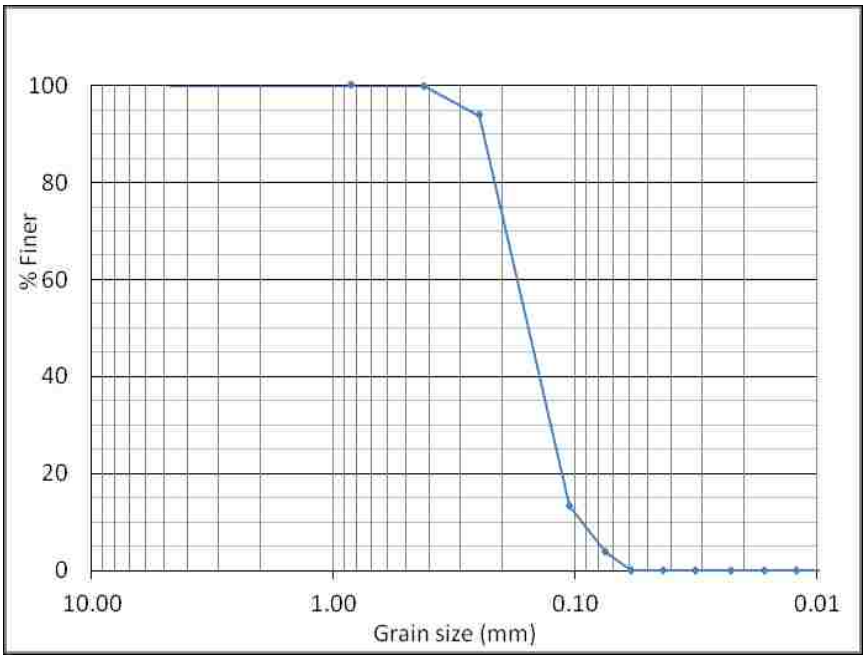

Figure 54. Site 4, layer 2

www.manaraa.com

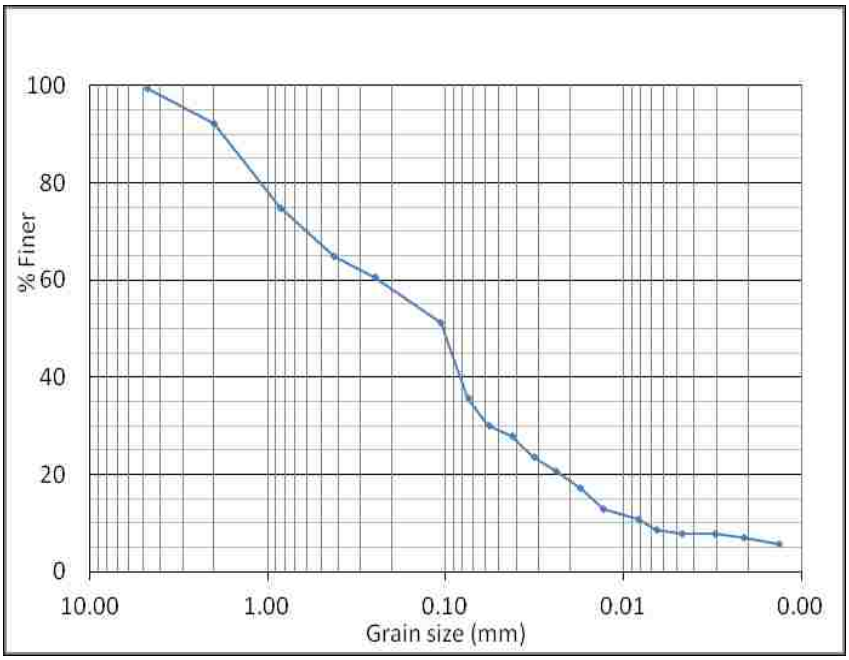

Figure 55. Site 4, layer 3

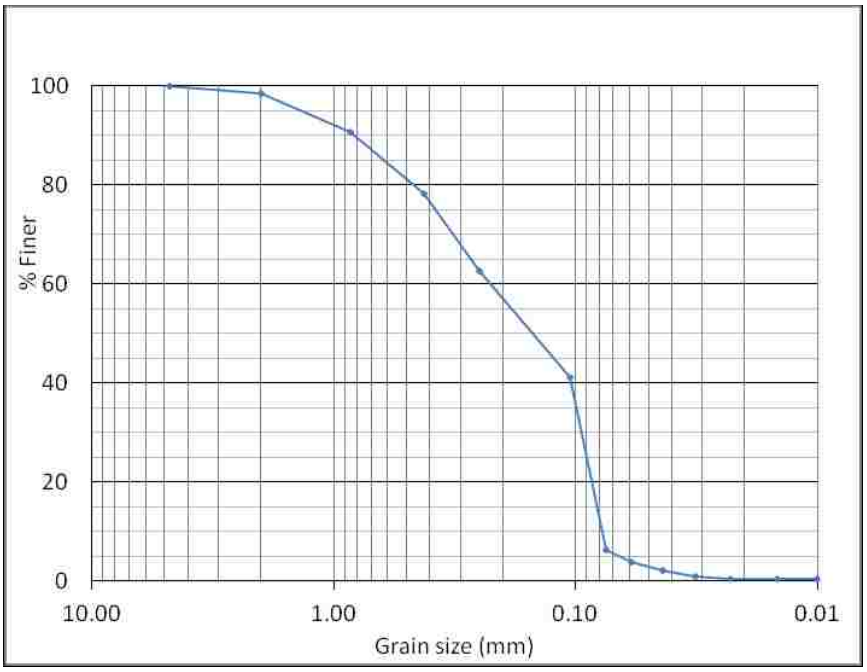

Figure 56. Site 4, layer 4

www.manaraa.com

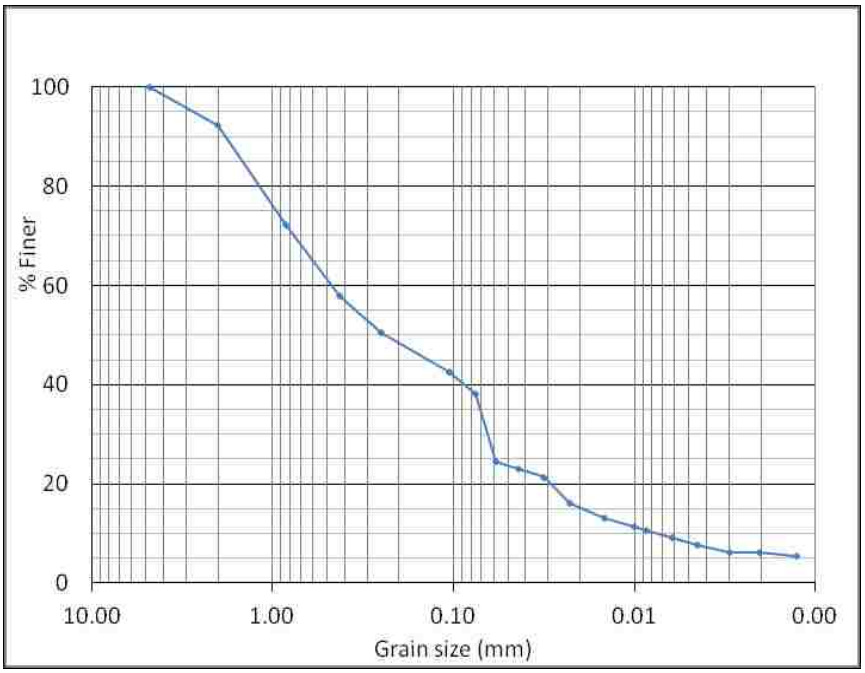

Figure 57. Site 4, layer 5

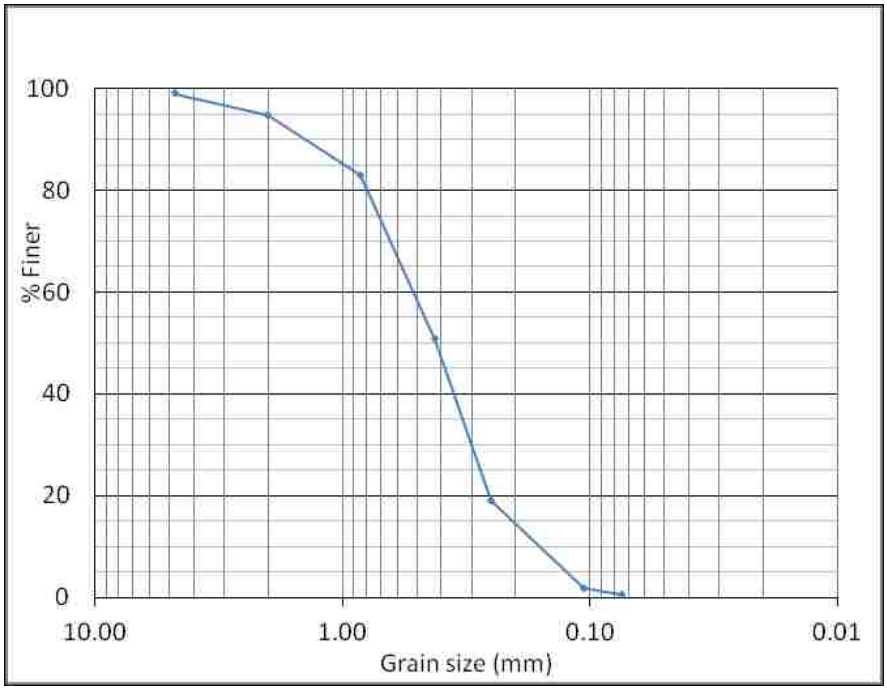

Figure 58. Site 4, layer 6

Horizontal hydraulic conductivity tests were completed on all layers that were greater than 2.5" thick. Since the soil compositions of the in situ cores were unknown, a constant

www.manaraa.com

head permeability tests was initially administered to all of the samples. Those samples that either took extended periods of time to saturate, or recorded results of conductivity values less than 10^{-3} cm/sec were switched to falling head permeability tests. The methods applied to the constant head and falling head permeability tests were taken from ASTM standards 2434 and 5856 respectively. The results for the constant head tests are displayed in figures to establish the linear relationship between the Darcy velocity and the hydraulic gradient to ensure laminar flow conditions. The falling head test results are displayed in tables.

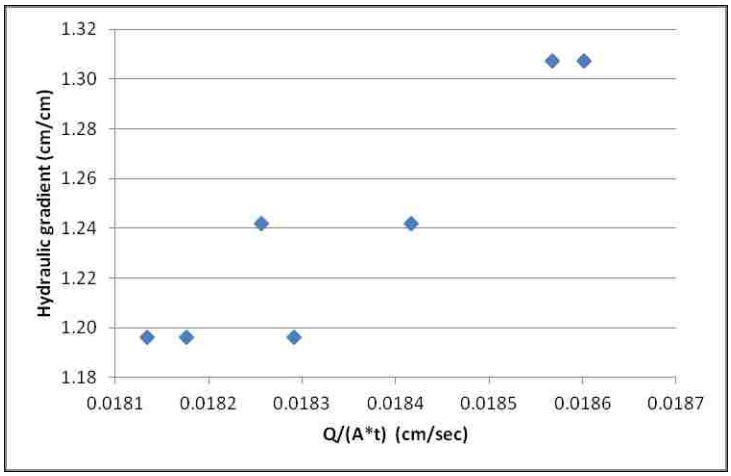

Figure 59. Site 1, layer 2

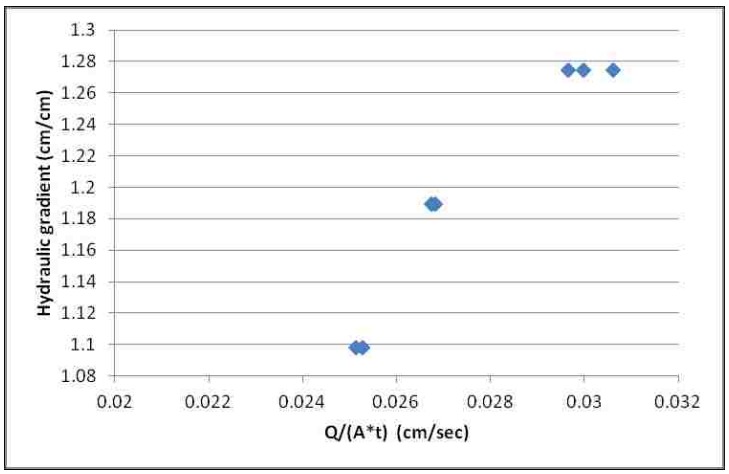

Figure 60. Site 1, layer 4

www.manaraa.com

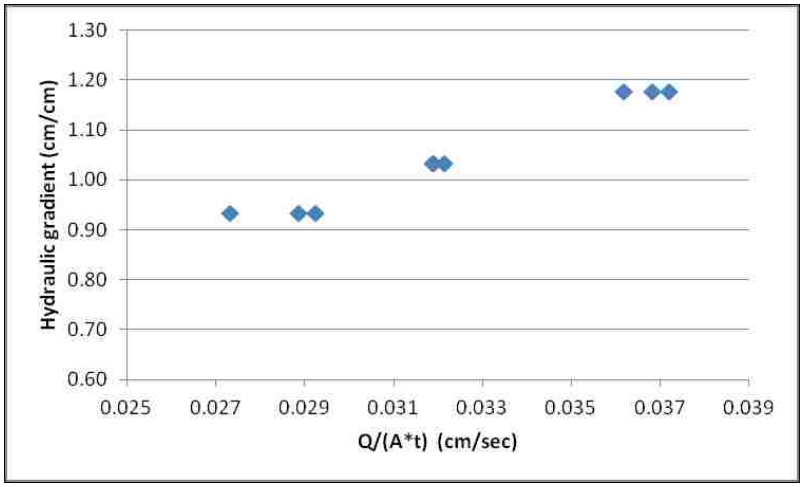

Figure 61: Site 2, organic surface layer

Table 7: Site 2, layer 1

	1	2	3
Beginning head difference (cm)	83.1	84.1	84.1
Ending head difference (cm)	59.9	31.1	62.3
Test duration (sec)	6810	21443	7373
Temp, T (°C)	22	22	22
Volume of water flow through specimen (cm^3)	117.56	268.55	110.46
Area of specimen, A (cm^2)	29.61	29.61	29.61
Hydraulic conductivity, K (cm/sec)	0.00013	0.00012	0.00011

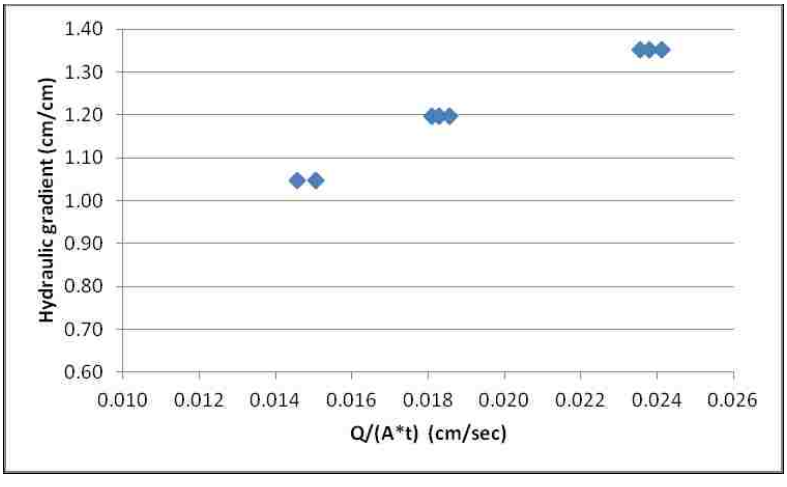

Figure 62. Site 2, layer 2

www.manaraa.com

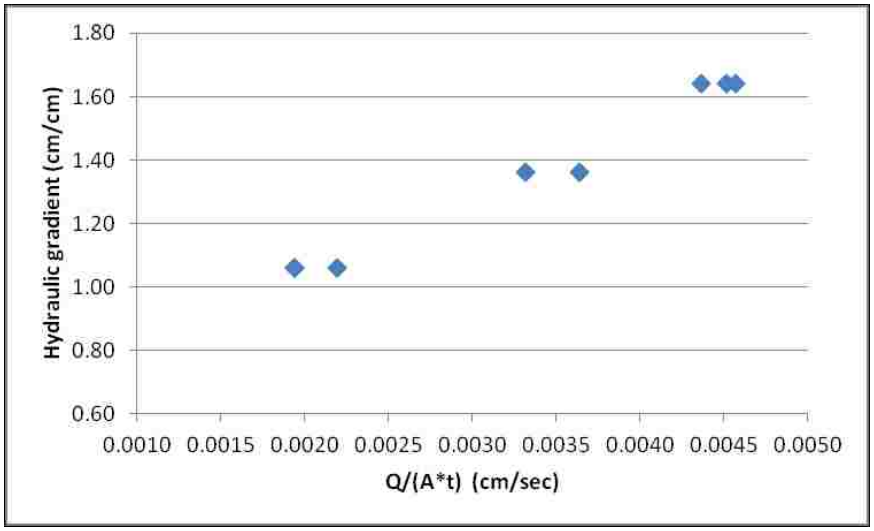

Figure 63. Site 2, layer 3

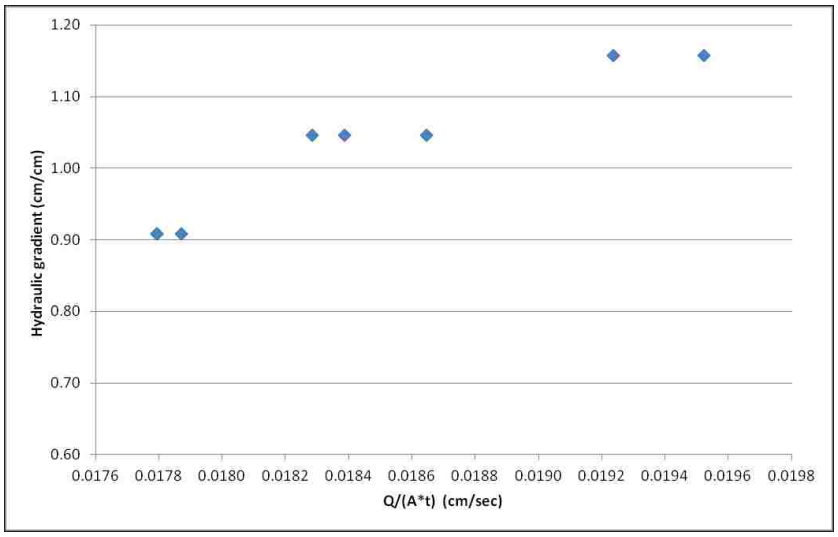

Figure 64. Site 2, layer 4

www.manaraa.com

Table 8: Site 3, layer 1

	1	2	3	4
Beginning head difference (cm)	80.8	80.8	80.8	81
Ending head difference (cm)	56.3	25.7	25.7	32.1
Test duration (sec)	3694	8586	10365	8364.000
Temp, T (°C)	22	22	22	22
Volume of water flow through specimen (cm^3)	124.14	279.20	279.20	247.78
Area of specimen, A (cm^2)	29.61	29.61	29.61	29.61
Hydraulic conductivity, K (cm/sec)	0.00026	0.00035	0.00029	0.00029

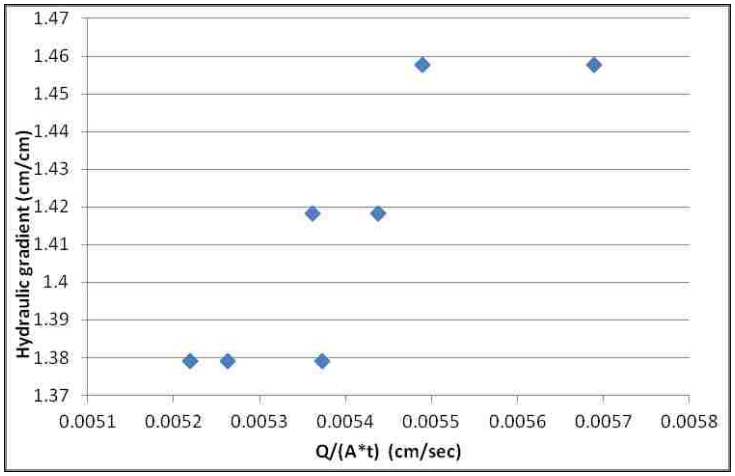

Figure 65. Site 3, layer 2

Table 9: Site 3, layer 3

	1	2	3
Beginning head difference (cm)	79.1	74.2	82.2
Ending head difference (cm)	43.2	24.6	59.1
Test duration (sec)	11371	21443	7373
Temp, T (°C)	22	22	22
Volume of water flow through specimen (cm^3)	181.91	251.33	117.05
Area of specimen, A (cm^2)	29.61	29.61	29.61
Hydraulic conductivity, K (cm/sec)	0.00014	0.00013	0.00012

www.manaraa.com

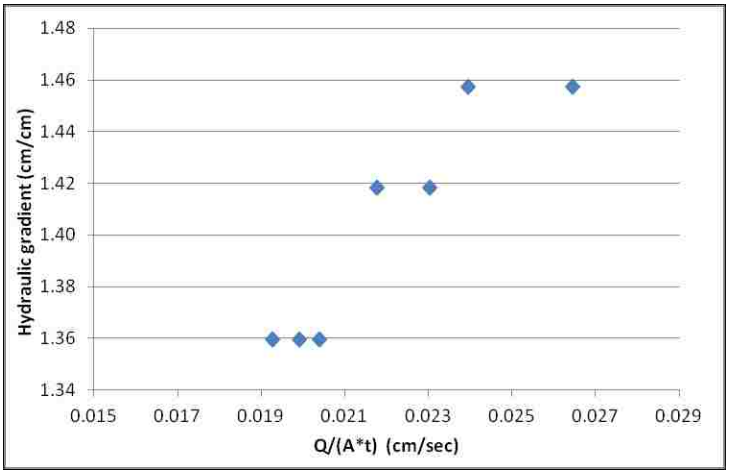

Figure 66. Site 3, layer 4

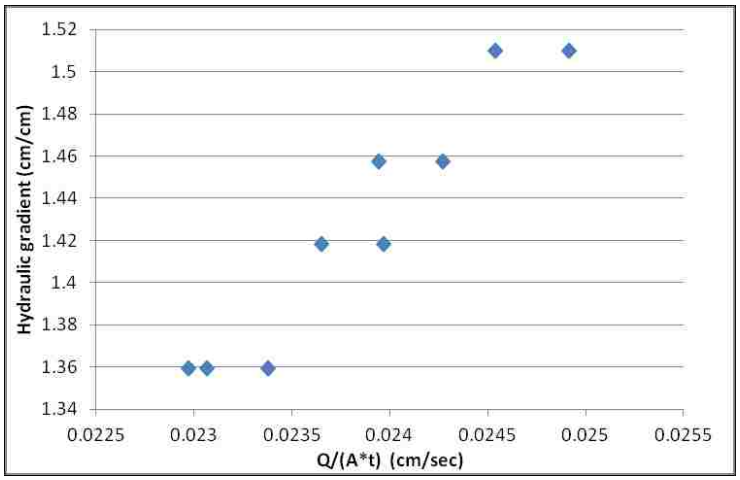

Figure 67. Site 3, layer 6

Table 10: Site 4, layer 1

	1	2	3
Beginning head difference (cm)	89.2	88.5	83.8
Ending head difference (cm)	49.5	39.9	52.4
Test duration (sec)	11371	16872	9891
Temp, T (°C)	22	22	22
Volume of water flow through specimen (cm^3)	201.16	246.26	159.11
Area of specimen, A (cm^2)	29.61	29.61	29.61
Hydraulic conductivity, K (cm/sec)	0.00014	0.00012	0.00012

www.manaraa.com

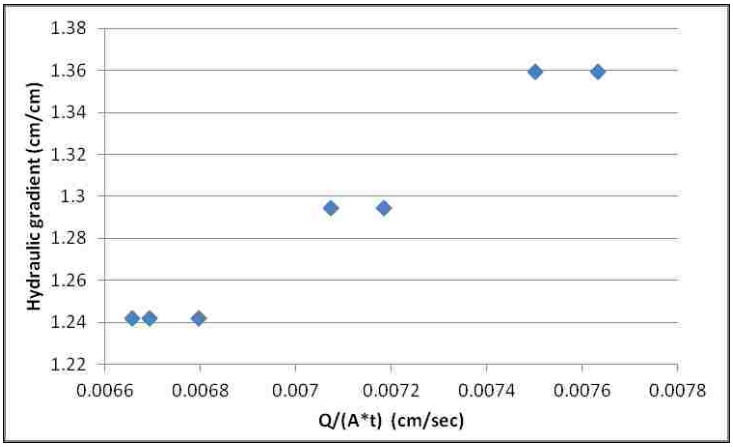

Figure 68. Site 4, layer 2

Table 11: Site 4, layer 3

	1	2	3
Beginning head difference (cm)	84.3	84.1	84.1
Ending head difference (cm)	52	31.1	62.3
Test duration (sec)	11371	21443	7373
Temp, T (°C)	22	22	22
Volume of water flow through specimen (cm^3)	163.67	268.55	110.46
Area of specimen, A (cm^2)	29.61	29.61	29.61
Hydraulic conductivity, K (cm/sec)	0.00011	0.00012	0.00011

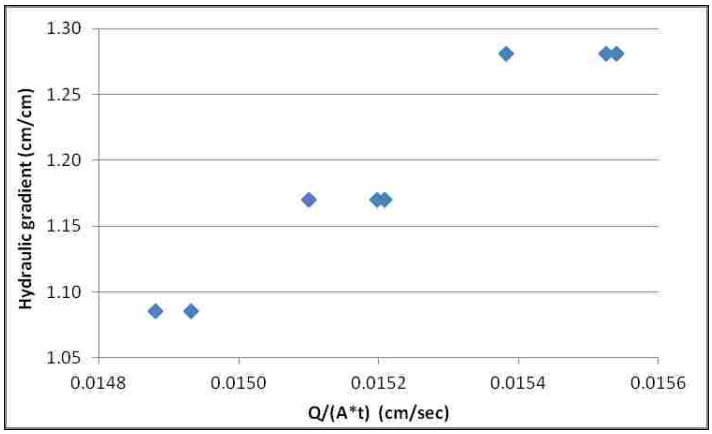

Figure 69. Site 4, layer 4

www.manaraa.com

Table 12: Site 4, layer 5

Beginning head difference (cm)	81.5
Ending head difference (cm)	76.6
Test duration (sec)	69565
Temp, T (°C)	22
Volume of water flow through specimen (cm^3)	24.83
Area of specimen, A (cm^2)	29.61
Hydraulic conductivity, K (cm/sec)	0.000002334

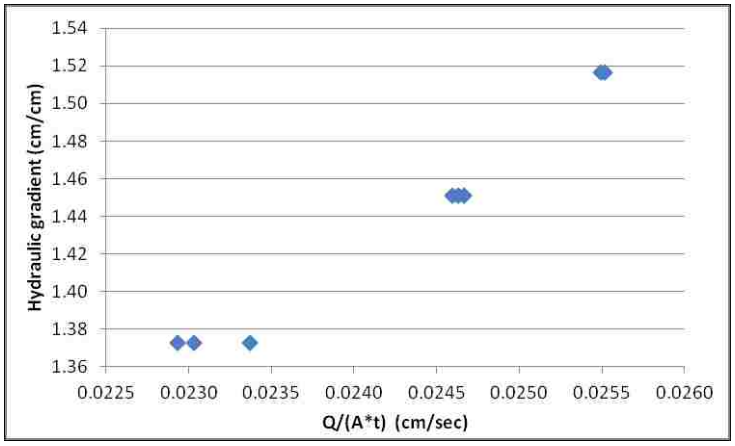

Figure 70. Site 4, layer 6

Water retention curves were completed for 6 samples. Three samples each from site 1 and site 4. Intact samples couldn't be retrieved from sites 2 and 3 because of the roots and because of the dry conditions, respectively. A 2.54 cm thick ring with a diameter of 6.35 cm was used for this test. The red sections were completed using a hanging column. The blue were completed using a pressure plate, and the yellow were completed using a WP-4 instrument. The data obtained through these tests were input into RETC to determine the α and n values used in HYDRUS to solve the Richard's Equation for unsaturated flow. These are included on the figures.

www.manaraa.com

Table 13: Site 1, layer 1

Sample 2				
Mass with rings and mesh (g)	Mass of sample (g)	Gravimetric	Volumetric	Suction (cm)
260	175.88	0.34	0.49	0.1
259.8	175.68	0.34	0.49	5
259.4	175.28	0.34	0.48	10
258.79	174.67	0.34	0.48	15
258.1	173.98	0.34	0.48	25
257.66	173.54	0.33	0.48	35
253.91	169.79	0.32	0.45	50
251.09	166.97	0.31	0.44	70
248.18	164.06	0.30	0.42	100
243.18	159.06	0.27	0.39	125
239.81	155.69	0.26	0.37	150
235.21	151.09	0.24	0.33	180
224.76	140.64	0.18	0.25	300
222.21	138.09	0.16	0.23	500
219.88	135.76	0.15	0.21	1000
219.35	134.1	0.14	0.20	2250
219.01	133	0.13	0.19	3750
218.84	131.9	0.12	0.18	6000
12.19	10.87	0.12	0.17	10000
12.95	11.53	0.12	0.17	15000
8.62	7.71	0.12	0.17	39768.3
9.63	8.59	0.12	0.17	99726.66
11.73	10.47	0.12	0.17	217196.1

Table 14: Site 1, layer 3

Sample 3				
Mass with rings and mesh (g)	Mass of sample (g)	Gravimetric	Volumetric	Suction (cm)
230.23	148.02	0.32	0.45	0.1
228.73	146.52	0.30	0.43	5
227.88	145.67	0.30	0.42	10
227.18	144.97	0.29	0.41	15
224.73	142.52	0.27	0.38	25.5
223.30	141.09	0.26	0.36	35
219.95	137.74	0.23	0.32	50
211.22	129.01	0.15	0.21	75
207.93	125.72	0.12	0.17	100
206.37	124.16	0.11	0.15	125
205.72	123.51	0.10	0.14	150
205.17	122.96	0.09	0.13	180
204.43	122.22	0.09	0.13	300
218.20	122.05	0.09	0.12	500
204.20	121.99	0.09	0.12	1000
203.85	121.64	0.08	0.118	2250
203.60	121.39	0.08	0.115	3750
204.30	121.42	0.08	0.115	6000
13.12	12.14	0.08	0.115	32732.37
12.87	11.9	0.08	0.116	63824.63
9.97	9.21	0.08	0.117	100455.3
11.51	10.65	0.08	0.115	164381.4
10.43	9.68	0.08	0.110	238454.5

www.manaraa.com

Table 15: Site 1, layer 4

Sample 1				
Mass with rings and mesh (g)	Mass of sample (g)	Gravimetric	Volumetric	Suction (cm)
242.34	161	0.26	0.39	0.1
235.45	154.11	0.23	0.34	5
231.75	150.41	0.21	0.31	10
229.48	148.14	0.20	0.29	15
222.21	140.87	0.15	0.23	30
219.54	138.2	0.14	0.21	37
216.69	135.35	0.12	0.18	49
209.68	128.34	0.07	0.11	74
207.31	125.97	0.05	0.08	100
206.31	124.97	0.05	0.07	125
205.87	124.53	0.04	0.07	150
205.48	124.14	0.04	0.06	180
205.31	123.97	0.04	0.06	300
205.21	123.74	0.04	0.06	500
205.01	123.67	0.04	0.06	1000
204.63	123.29	0.03	0.05	2250
204.38	123.04	0.03	0.05	3750
204.3	122.96	0.03	0.05	6000
11.419	11.1	0.028738739	0.04	10000
10.999	10.7	0.027943925	0.04	25084.62
11.183	10.9	0.025963303	0.04	80000
9.643	9.4	0.025851064	0.04	161112.6
11.387	11.1	0.025855856	0.04	199861.2

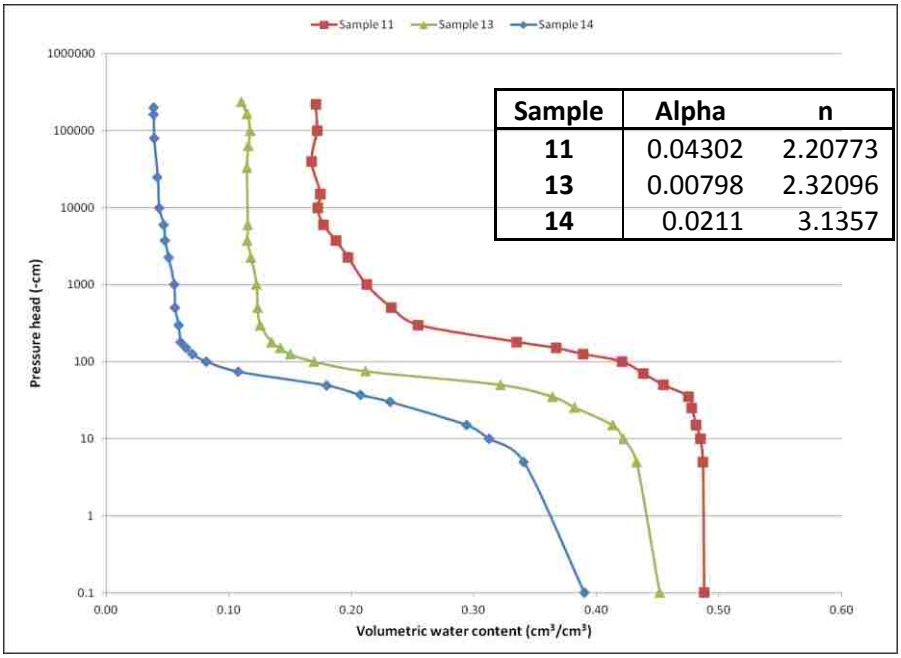

Figure 71. Water retention curve for site 1

www.manaraa.com

Table 16: Site 4, layer 1

Sample 41				
Mass with rings and mesh (g)	Mass of sample (g)	Gravimetric	Volumetric	Suction (cm)
249.4	167.39	0.289682777	0.443214648	0.01
248.8	166.79	0.287127526	0.439305114	5
247.9	165.89	0.283259992	0.433387787	15
243.71	161.7	0.264687693	0.404972171	30
239.61	157.6	0.245558376	0.375704315	50
230.91	148.9	0.201477502	0.308260578	75
220.75	138.74	0.143001297	0.218791985	100
218.17	136.16	0.126762632	0.193946827	125
217.34	135.33	0.121406931	0.185752605	150
216.15	134.14	0.113612644	0.173827345	175
214.55	132.54	0.102912328	0.157455862	500
213.98	131.97	0.09903766	0.15152762	1000
212.12	130.11	0.086157866	0.131821536	2250
211.87	129.86	0.084398583	0.129129832	3750
211.18	129.17	0.079507626	0.121646667	6000
9.91	9.21	0.076004343	0.116286645	23555.07
11.43	10.6	0.078301887	0.119801887	44153.01
12.54	11.65	0.07639485	0.11688412	95545.89
12.83	11.92	0.076342282	0.116803691	194762.7
13.98	13.03	0.072908672	0.111550269	268181.1

Table 17: Site 4, layer 3

Sample 43				
Mass with rings and mesh (g)	Mass of sample (g)	Gravimetric	Volumetric	Suction (cm)
225.1	144.02	0.283363422	0.402376059	0.01
224.5	143.42	0.28036536	0.398118812	4
211.97	130.89	0.211475285	0.300294904	15
207.7	126.62	0.184883905	0.262535145	30
205.2	124.12	0.168466001	0.239221721	50
203.81	122.73	0.159048317	0.225848611	75
203.46	122.38	0.156643242	0.222433404	100
200.93	119.85	0.138840217	0.197153108	125
199.58	118.5	0.129029536	0.183221941	150
199.33	118.25	0.127188161	0.180607188	175
198.76	117.68	0.122960571	0.174604011	500
197.89	116.81	0.116428388	0.165328311	1000
197.12	116.04	0.110565322	0.157002758	2250
196.55	115.47	0.106174764	0.150768165	3750
196.76	115.68	0.107797372	0.153072268	6000
10.11	9.13	0.107338445	0.152420591	19374.3
9.89	8.94	0.106263982	0.150894855	73418.4
11.41	10.31	0.106692532	0.151503395	108190.17
12.97	11.71	0.107600342	0.152792485	207406.98
12.56	11.36	0.105633803	0.15	347717.7

www.manaraa.com

Table 18: Site 4, layer 4

Sample 44				
Mass with rings and mesh (g)	Mass of sample (g)	Gravimetric	Volumetric	Suction (cm)
225.11	141.81	0.24476412	0.34	0.01
220.98	137.68	0.22210924	0.31	4
214.87	131.57	0.18598465	0.26	15
208.9	125.6	0.14729299	0.20	30
202.91	119.61	0.10458992	0.15	50
198.13	114.83	0.0673169	0.09	75
197.11	113.81	0.05895791	0.08	100
196.41	113.11	0.05313412	0.07	125
195.89	112.59	0.04876099	0.07	150
195.35	112.05	0.04417671	0.06	175
195.15	111.85	0.04246759	0.06	500
194.88	111.58	0.04015056	0.06	1000
194.78	111.48	0.03928956	0.05	2250
194.61	111.31	0.0378223	0.05	3750
194.6	111.3	0.03773585	0.05	6000
12.3	11.82	0.04060914	0.06	9279.27
11.3	10.88	0.03860294	0.05	19374.3
9.9	9.56	0.03556485	0.05	59856.39
9.76	9.42	0.03609342	0.05	93812.4
10.91	10.51	0.03805899	0.05	164375.64

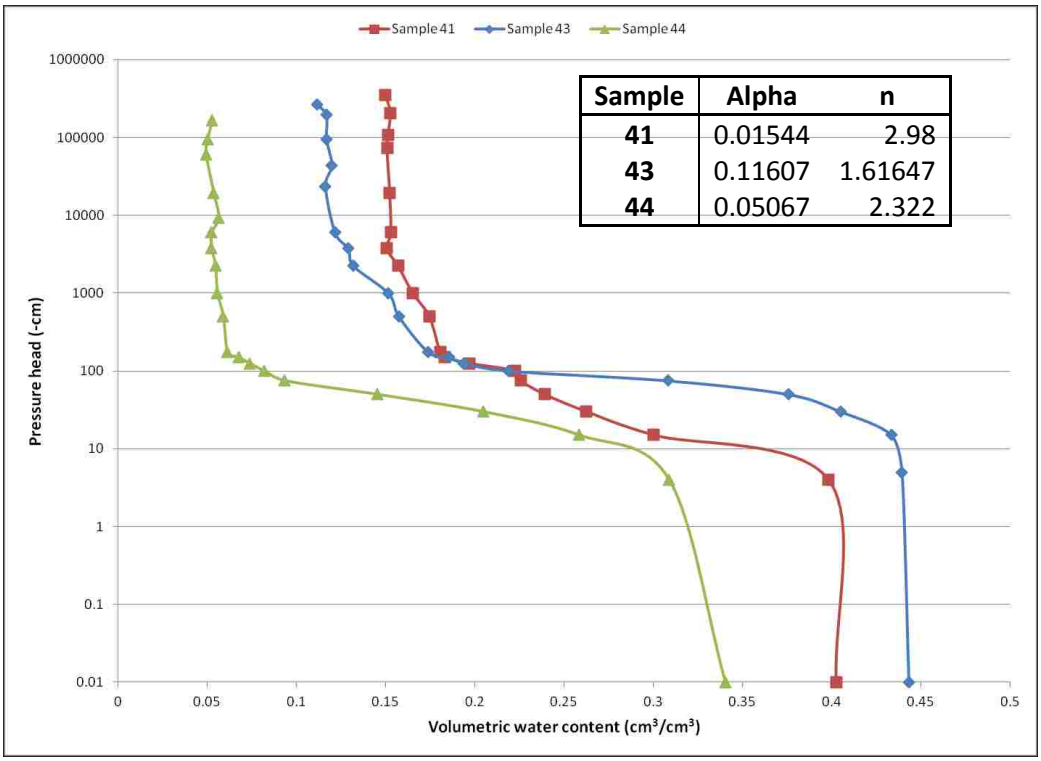

Figure 72. Water retention curve for site 4

www.manaraa.com

The final data to be included here is a qualitative study of the cores obtained by the USGS during the installation of the wells at the Rio Bravo site. The NRCS flow diagram in Figure 73 was used for this analysis. The key objective of this analysis was to identify low permeability layers that may have had an impact on the model calibration. The results are included below.

Table 19. Results for the analysis of the USGS East River well core

Depth (ft)	Soil Texture
6-8	coarse sand with gravel
9-13	sand
13-17	missing
17-25	coarse sand
25-26	silty clay
26-29	fine sand
29-31	silty clay loam
31-35	silty clay
35-36	missing
36-38	clay loam
38-40	coarse sand with gravel
40-42	coarse sand
42-44	gravel
44-48	sand
46-48	gravel
48-50	sand
50-52	gravel

Table 20. Results for the analysis of the USGS East Bosque well core

Depth (ft)	Soil Texture
6-10	missing
10-20	coarse sand with gravel
20-24	coarse sand with no gravel
24-25	sandy clay loam
25-29	missing
29-32	loamy sand
32-33	coarse gravel with sand
33-34	missing
34-36	silty clay loam
36-42	large gravel (>2") and sand
42-48	sand
48-50	coarse gravel with sand

www.manaraa.com

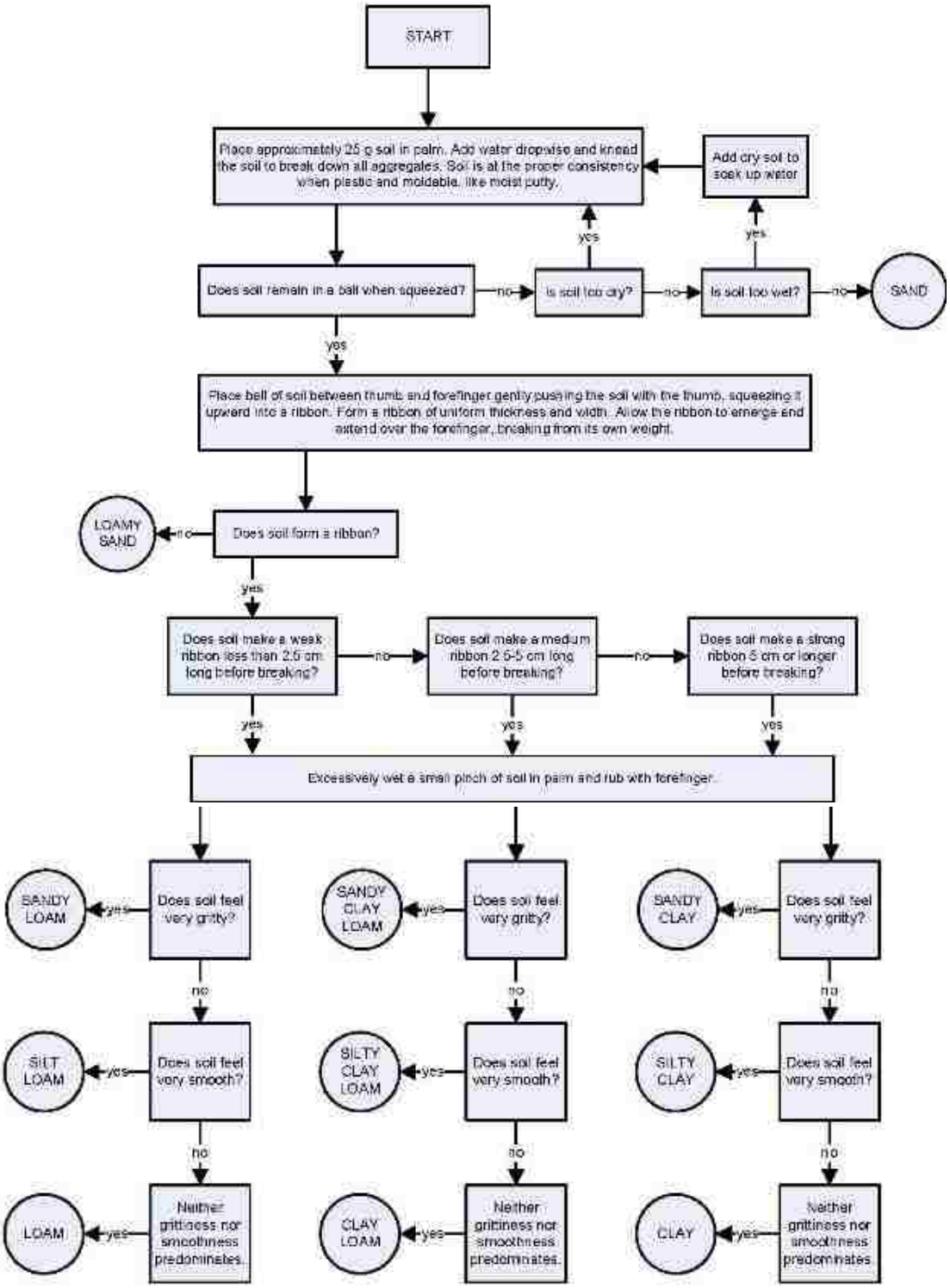

Figure 73. NRCS soil texture classification flow chart

www.manaraa.com

Appendix F: Model results

The majority of the model results obtained through the analyses is included above. The figures that are included here detail the analyses completed for each of the 6 primary flood events, which include the storage and fluxes for each individual layer.

Table 21. Rio Bravo data

	Time to saturation	Maximum flux ($cm^3/s•m$)	Volume of water stored (m^3/m)	Time to release
Upper Level				
Layer 1	4 hrs	2.09	0.0895	10 hrs
Layer 2	5 hrs	6.85	0.1156	14 hrs
Layer 3	4 hrs	1.44	0.026	11 hrs
Layer 4	5 hrs	1.96	0.009	8 hrs
Layer 5	7 hrs	12.745	0.091	11 hrs
Layer6	10 hrs	235.43	6.015	39 hrs
Lower Level				
Layer 1	3 hrs	0.73736	0.21316	39 hrs
Layer 2	3 hrs	10.22	0.809	40 hrs
Layer 3	3 hrs	12.402	0.37684	41 hrs

Table 22. Rio Bravo 2-day data

	Time to saturation	Maximum flux ($cm^3/s•m$)	Volume of water stored (m^3/m)	Time to release
Upper Level				
Layer 1	5 hrs	2.1132	0.0918	16 hrs
Layer 2	52 hrs	6.5096	0.1769	60 hrs
Layer 3	51 hrs	1.5293	0.058	61 hrs
Layer 4	52 hrs	1.7159	0.13	61 hrs
Layer 5	52 hrs	13.768	0.2646	61 hrs
Layer6	55 hrs	280.45	14.396	116 hrs
Lower Level				
Layer 1	3 hrs	4.2009	0.45082	93 hrs
Layer 2	3 hrs	29.144	0.8053	100 hrs
Layer 3	3 hrs	9.0729	0.30616	100 hrs

www.manaraa.com

Table 23. Rio Bravo 10-day data

	Time to saturation	Maximum flux ($cm^3/s•m$)	Volume of water stored (m^3/m)	Time to release
Upper Level				
Layer 1	5 hrs	2.088	0.0901	18 hrs
Layer 2	12 hrs	6.8105	0.1579	114 hrs
Layer 3	59 hrs	1.563	0.062	156 hrs
Layer 4	57 hrs	1.9399	0.121	141 hrs
Layer 5	32 hrs	12.85	0.23	184 hrs
Layer6	242 hrs	250.88	18.232	312 hrs
Lower Level				
Layer 1	3 hrs	0.7172	0.2133	276 hrs
Layer 2	3 hrs	8.8307	0.8102	278 hrs
Layer 3	3 hrs	11.718	0.378	279 hrs

Table 24. Alameda data

	Time to saturation	Maximum flux ($cm^3/s•m$)	Volume of water stored (m^3/m)	Time to release
Upper Level				
Layer 1	5 hrs	2.1169	0.1143	13 hrs
Layer 2	7 hrs	11.096	0.3057	19 hrs
Layer 3	12 hrs	2.9064	0.071	24 hrs
Layer 4	12 hrs	9.8158	0.169	25 hrs
Layer 5	10 hrs	13.011	0.2376	19 hrs
Layer6	15 hrs	282.82	9.287	56 hrs
Lower Level				
Layer 1	3 hrs	3.945	0.44974	46 hrs
Layer 2	3 hrs	27.711	0.7978	52 hrs
Layer 3	3 hrs	8.6325	0.3045	52 hrs

Table 25. Alameda 2-day data

	Time to saturation	Maximum flux ($cm^3/s•m$)	Volume of water stored (m^3/m)	Time to release
Upper Level				
Layer 1	4hrs	2.1125	0.1143	22 hrs
Layer 2	55 hrs	11.249	0.7502	73 hrs
Layer 3	56 hrs	3.4109	0.393	91 hrs
Layer 4	56 hrs	9.8269	0.937	92 hrs
Layer 5	50 hrs	10.99	0.4573	68 hrs
Layer6	59 hrs	279.6	19.058	135 hrs
Lower Level				
Layer 1	2 hrs	4.1497	0.4481	94 hrs
Layer 2	2 hrs	28.732	0.806	105 hrs
Layer 3	2 hrs	8.9957	0.3061	106 hrs

www.manaraa.com

Table 26. Alameda 10-day data

	Time to saturation	Maximum flux ($cm^3/s•m$)	Volume of water stored (m^3/m)	Time to release
Upper Level				
Layer 1	6 hrs	2.1068	0.1142	38 hrs
Layer 2	233 hrs	10.936	1.2848	265 hrs
Layer 3	159 hrs	3.5046	0.548	330 hrs
Layer 4	156 hrs	10.061	1.249	276 hrs
Layer 5	107 hrs	12.844	0.5091	254 hrs
Layer6	242 hrs	247.36	25.77	333 HRS
Lower Level				
Layer 1	3 hrs	0.9201	0.2134	268 hrs
Layer 2	3 hrs	11.455	0.8103	274 hrs
Layer 3	3 hrs	12.741	0.378	278 hrs

www.manaraa.com

Works Cited

Association of State Floodplain Managers (2008). *Floodplain Management-More than flood loss reduction.* Madison, WI: ASFM.

Barlow, P. M, DeSimone, L.A., and Moench, A.F. (2000). Aquifer response to stream-stage and recharge variations ll. Convolution method and applications. *Journal of Hydrology* , 211-229.

Bartolino, J. R. and Cole, J. C. (2002). *Ground-Water Resources of the Middle Rio Grande Basin, New Mexico.* U.S. Geological Survey Circular 1222.

Bartolino, J. R. and Niswonger, R. G. (1999). *Numerical simulation of vertical ground water flux of the Rio Grande from ground-water temperature profiles, central New Mexico.* Albuquerque: Water resources investigations report 99-4212.

Bates, P. D., Stewart, M. D., Desitter, A., Anderson, M. G., Renaud, J. P., and Smith, J. A. (2000). Numerical solution of floodplain hydrology. *Water Resources Research* , 2517-2529.

Chen, X. C., Chen D. Y. and Chen, X. (2006). Simulation of baseflow accounting for the effect of bank storage and its implication in baseflow separation. *Journal of Hydrology* , 539-549.

Connell, S. D. (2007). *Geomorphology and stratigraphy of inset fluvial deposits along the Rio Grande valley in the central Albuquerque Basin, New Mexico.* Albuquerque, NM: New Mexico Bureau of Geology and Mineral Resources.

Cooper Jr., H. H. and Rorabaugh, M. I. (1963). Ground water movements and bank storage due to flood stages in surface streams. *USGS Water Supply Paper 1536-J* , 339-366.

Daniels, J. M. (2003). Floodplain aggradation and pedogenesis in a semiarid environment. *Geomorphology* , 225-242.

de Groot, R. S., Wilson, M. A., and Boumans, R. M. J. (2002). A typology for the classification, description, and valuation of ecosystem functions, goods and services. *Ecological Economics* , 393-408.

Engdahl, N. B. and Weissmann, G. S. (2010a). Anisotropic transport rates in heterogeneous porous media. *Water Resources Research* , 1-12.

Engdahl, N. B., Vogler, E. T., and Weissmann, G. S. (2010b). Evaluation of aquifer heterogeneity effects on river flow loss using a transition probabilty framework. *Water Resources Research* , 1-12.

Hantush, M. M., Harada, M., and Marino, M. A. (2002). Hydraulics of stream flow routing with bank storage. *Journal of Hydrologic Engineering* , 76-89.

Hunt, B. (1990). An approximation for the bank storage effect. *Water Resources Research* , 2769-2775.

www.manaraa.com

Hunt, B. (2005). Bank-storage problem and the dupuit approximation. *Journal of Hydrologic Engineering* , 118-124.

Li, H., Boufadel, M. C., and Weaver, J. W. (2008). Quantifying bank storage of variably saturated aquifers. *Ground Water* , 841-850.

Maddock, I. (1999). The importance of physical habitat assessment for evaulating river health. *Freshwater Biology* , 373-391.

Makar, P. M., Massong, T., and Bauer, T. (2006). *Channel widths changes along the Middle Rio Grande, NM.* Albuquerque: Bureau of Reclamation.

Moench, A. F., Sauer, V. B., and Jennings, M. E. (1974). Modification of routed streamflow by channel loss and base-flow. *Water Resources Research* , 963-968.

Molles Jr., M. C., Crawford, C., Ellis, L. M., Valett, H. M., and Dahm, C. N. (1998). Managed flooding for riparian ecosystem restoration. *Bioscience* , 749-756.

Morel-Seytoux, H. J. (1975). A combined model of water table and rive stage evolution. *Water Resources Research* , 968-972.

MRGCD. (2012.). *The Rio Grande: A ribbon of life and tradition.* Retrieved June 25, 2012, from Middle Rio Grande Conservancy District web site: www.mrgcd.com/History.aspx

Myers, N. (2010). *Slug-test package for inner valley alluvium adjacent to the Rio Grande in Albuquerque, NM.* Albuquerque: NM Water Science Center.

Neuman, S.P., Witherspoon, P.A., (1970). Finite element method of analyzing steady seepage with a free surface, *Water Resources Research*, 6, 889–897.

Neuman, S.P., Witherspoon, P.A., 1970. Variational principles for confined and unconfined flow of groundwater, *Water Resources Research*, 6, 1376–1382.

Neuman, S.P., Witherspoon, P.A., 1971. Analyzing nonsteady flow with a free surface using the finite element method, *Water Resources Research*, 7, 611–623.

Pinder, G. F. and Sauer, S. P. (1971). Numerical solution of flood wave modification due to banks storage effects. *Water Resources Research* , 63-70.

Rankin, D. R., McCoy, K. J., Geoff, J. M., Worthington, J. A., and Bandy-Baldwin, K. M. (2011). *Groundwater hydrology and estimation of horizontal groundwater flux from the Rio Grande at selected locations in Albuqerque, New Mexico, 2008-1010.* Scientific Investigations Report 2011-XXXX.

Rorabaugh, M. J. (1963). Estimating changes in bank storage and ground-water contribution to stream-flow. *International Association of Scientific Hydrology* , 432-441.

Sharp Jr., J. M. (1977). Limitations of bank storage model assumptions. *Journal of Hydrology* , 31-47.

www.manaraa.com

Sophocleous, M. (2002). Interactions between groundwater and surface water: the state of the science. *Hydrogeology Journal* , 52-67.

Squillace, P. J. (1996). Observed and simulated movement of bank storage water. *Ground Water* , 121-134.

Tetra Tech Inc. (2004). *Habitat Restoration Plan for the Middle Rio Grande.* Albuquerque, NM: Middle Rio Grande Endangered Species Act Collaborative Program.

Thompson, S. (2003). *Using HYDRUS-2D to model tree belts for salinity and recharge control.* Thesis. The Univesity of Western Australia.

Todd, D. K. (1955). *Ground water flow in relation to a flooding stream.* New York: American Society of Civil Engineers.

Whiting, P. J., and Pomeranets, M. (1997). A numerical study of bank storage and its contribution to streamflow. *Journal of Hydrology* , 121-136.

Wilson, M. A. and Carpenter, S. R. (1999). Economic valuation of freshwater ecosystem services in the United States. *Ecological Applications* , 772-783.

Wyman, S. (2007). *Saltcedar (Tamarix).* National Riparian Service Team (NSRT).

Zitta, V. L. and Wiggert, J. M. (1971). Flood routing in channels with bank seepage. *Water Resources Research* , 1341-1345.

www.manaraa.com